Stony Brook University

Quantifying Atlantic menhaden in estuarine and coastal waters of Long Island, New York using acoustic methods.

A Thesis Presented

by

Brandyn Mark Lucca

to

The Graduate School

in Partial Fulfillment of the

Requirements

for the Degree of

Master of Science

in

The School of Marine and Atmospheric Sciences

Stony Brook University

December 2016

Stony Brook University

The Graduate School

Brandyn M. Lucca

We, the thesis committee for the above candidate for the

Master of Science degree, hereby recommend

acceptance of this thesis.

Joseph D. Warren – Thesis Advisor
Associate Professor, School of Marine and Atmospheric Sciences, Stony Brook University

Bradley J. Peterson – First Reader
Associate Professor, School of Marine and Atmospheric Sciences, Stony Brook University

Kevin M. Boswell – Second Reader
Assistant Professor, Department of Biological Sciences, Florida International University

This thesis is accepted by the Graduate School

Charles Taber

Dean of the Graduate School

Abstract of the Thesis

Quantifying Atlantic menhaden in estuarine and coastal waters of Long Island, New York using acoustic methods.

by

Brandyn Mark Lucca

Master of Science

in

The School of Marine and Atmospheric Sciences

Stony Brook University

2016

Forage fish are an ecological cornerstone that trophically link primary production with pelagic predators such as piscivorous fish, marine mammals, seabirds, and humans. Atlantic menhaden (*Brevoortia tyrannus*) are one such forage fish species that can be found in both estuarine and coastal waters from the Gulf of Maine to Florida throughout the year. Alongside their ecological importance as prey for commercially important species such as striped bass and bluefin tuna, menhaden are fished to be used as bait or reduced into oil. New York has an especially rich history with the commercial harvesting of menhaden beginning in the late 17th century. Despite their relative ecological and economic importance, there is a paucity of quantitative data that describes the spatial and temporal distributions of menhaden in many regions throughout their geographic range. A promising method to study the distribution of menhaden is active acoustics which has been utilized in other fisheries to provide relatively time-efficient quantitative data with broad spatial coverage and high resolution. Acoustic surveys were conducted in two different habitats (estuarine, coastal) where menhaden are found during the 2014 and 2015. Menhaden aggregations were very patchy and there was evidence of significant clustering in both habitats. Coastal menhaden abundance and biomass were relatively constant throughout the summer with a peak in the late-summer. Conversely, estuarine menhaden abundance and biomass biomass peaked in late-spring and early-fall, and decreased by three orders of magnitude by mid-fall. Mean target strength (TS) of coastal menhaden was relatively constant which suggested no differences in the size classes of fish. Conversely estuarine TS distributions shifted throughout the sampling effort which were consistent with changes in the size classes of fish as they grow and migrate in and out of the estuarine habitat. This study demonstrates that active acoustics is a viable tool for measuring menhaden abundance and biomass in both coastal and shallow-water (< 4 m) estuarine waters.

Table of Contents

Acknowledgments

I would like to thank my friends, family, and loved ones for supporting me during all of my course- and fieldwork. Additional thanks to my adviser, Dr. Joseph Warren, for guiding my growth as a graduate student and keeping an even keel when I made mistakes and my thesis readers, Dr. Bradley Peterson and Dr. Kevin Boswell, for using their time and effort to provide their expertise and insight. Lastly, I would like to thank everyone who provided assistance in the field, during classes, and/or maintaining my sanity: Erica Bedard, Captains Brian Gagliardi and Andrew Brosnan, Stephen Heck, Justin Lashley, Amanda Tinoco, Maija Niemisto, Samuel Urmy, Hannah Blair, Amber Subtler, Gina Clementi, Christopher Paparo, and many more. Thank you all.

Chapter 1

Acoustically-measured distribution and abundance of Atlantic menhaden (*Brevoortia tyrannus*) in a shallow estuary in Long Island, NY

Introduction

Atlantic menhaden (*Brevoortia tyrannus* Latrobe 1802) is a planktivorous forage fish that make large northward and southward migrations away from the coastal waters of North Carolina extending from Florida to Maine and constantly move in and out of coastal estuaries (Ahrenholz 1991; Nicholson 1978). Newly spawned larvae emigrate into these estuaries and rapidly metamorphose into juveniles and begin feeding mostly on zooplankton (Friedland *et al.* 2011; Reintjes 1969). Due to their relatively large size range located in these estuaries (from larvae to adults) menhaden are an important trophic link between estuarine primary productivity and pelagic piscivores such as striped bass (*Morone saxatalis*), bluefish (*Pomatomus saltarix*), coastal seabirds, and marine mammals (Ahrenholz, 1991).

Economically, menhaden are primarily fished to be used as bait or reduced for their oil (SEDAR 2015). The menhaden fishery was one of the largest in the United States before its collapse in the 1950's (McHugh 1972) and has been allowed to recover due to the combined efforts of the Atlantic States Marine Fisheries Commission (ASMFC) and state regulators. Historically, menhaden fishing began in New York during the early 17th century and played an important role in the state's economic and social development (Gabriel 1921; Goode 1880; Turrentine 1913). The Peconic Estuary in particular benefited local economies from historical menhaden fishing (Goode 1880; Senate Document 1878); however, due to its relative importance to both fishermen and environmentalists in New York, the menhaden fishery has a long-standing and contentious regulatory history which has fueled bitter public debate for nearly a century over proper management (Gabriel 1921; SEDAR 2015).

This estuary covers 218 km^2 and extends from the Peconic River to Long Island Sound and is an important habitat for a wide variety of marine animals such as shellfish, finfish, seabirds, and marine mammals (Bortman and Niedowski 1998; Hardy 1976). Habitats such as creeks, coastal marsh grass, and seagrass beds located throughout the estuary act as critical refuges for age-0 fish. Their presence in the western Peconic Estuary, the region comprising the Peconic River, Flanders Bay, and Reeves Bay, is especially notable due to their association with large fish kills (SCDHS 2016).

During the late spring and early summer of 2015, three large fish kills occurred were in the Peconic River. The Suffolk County Department of Health Services (SCDHS) concluded that the fish kills were the result of several concomitant factors resulting in low dissolved oxygen (< 1.0 mg/L) throughout the river and connecting creeks (SCDHS 2016). First, a large number of bluefish were observed chasing and subsequently trapping menhaden in the relatively shallow waters of the Peconic River. Second, blooms of three ichthyotoxic dinoflagellate species (*Gymnodinium instriatum*, *Prorocentrum minimum*, and *Karlodinium veneficum*) preceded the kills which were believed to have caused gill damage and exacerbated decreases in local dissolved oxygen. Both of these factors are not uncommon and regularly occur every year in this part of the estuary (O'Shea and Brosnan 2000; Wall *et al.* 2013; SCDHS 2016). Likewise, the sum of the 2015 estimated kill numbers (10,000s of fish killed on 16 May and 14 June and 200,000 for 27 May) were on the same order of magnitude as kills which occurred during 2008 and 2009 (SCDHS 2016), although the method used to produce these estimates was not described.

Although some fishery-independent surveys conducted by the New York State Department of Environmental Conservation (NYSDEC) in Peconic and Gardiners Bay from 1987 to 2013 (Bortman and Niedowski 1998; SEDAR 2015; Weber and Grahn 1995; Weber *et al.* 1998) have been incorporated into stock assessment models, they were not specifically targeted at menhaden and used a small-mesh trawl as opposed to purse seining (Smith 1991; Smith 1999). Moreover, the data collected from the NYSDEC has been primarily used to generate recruitment success and juvenile abundance indices (Bucheister *et al.* 2016; SEDAR 2015). Consequently, studies providing quantitative estimates for spatiotemporal distributions of menhaden abundance in the Peconic Estuary, let alone in Flanders Bay and the Peconic River, have not been done. One limiting factor in the western Peconic Estuary is the very shallow depths (< 4 m) and tidal ranges of approximately 1 meter both of which severely limit the size of vessels and amount of time available to conduct comprehensive net trawl studies. Likewise, purse seine surveys are limited to river banks. Therefore, methods that are capable of operating in very shallow waters and can provide quantitative data estimating spatial and seasonal menhaden abundances are needed to improve stock assessments and improve understanding of ecological mechanisms (e.g., predator-prey interactions).

While acoustic surveys have not been used previously to estimate the abundance of Atlantic menhaden, fishery acoustics has been an integral tool for effective fisheries management of other forage fish groups such as anchovy, sardine, and herring (Demer *et al.* 2013; Koslow 2009; Simmonds and MacLennan 2006). Compared to traditional sampling methods, fishery acoustics provides a time-efficient and non-invasive approach that provides data with high spatial and temporal resolution (Coasta *et al.* 2014). Moreover, the miniaturization of acoustic equipment allows for the use of smaller vessels capable of conducting shallow-water surveys (Fernandes *et al.* 2002). Active acoustic sampling using horizontal sampling echosounders has been previously used in shallow water estuaries such as those shallower than 2 m (Boswell *et al.* 2007), macrotidal mangroves (Krumme and Saint-Paul 2003), and rivers (Duncan and Kubecka, 1996). However, very few studies (Bezaerra-Neto *et al,* 2013) have used vertical sampling echosounders to sample very shallow waters with depths less than (< 2 m) but have been limited to freshwater systems. Compared to horizontal echosounders, other studies have observed that vertical echosounders may under-sample the presence of fish and underestimate numeric fish densities in shallow-water habitats by an order of magnitude (Kubecka and Wittingerova 1998) due to a combination of horizontal fish avoidance and being unable to subsequently measure them acoustically. Additional sampling techniques such as sidescan sonar can be used to provide complementary data in order to estimate fish school information that would otherwise be under-sampled using vertical echosounders (Simmonds and MacLennan 2006).

Providing quantitative estimates of menhaden abundance and biomass in the western Peconic Estuary with relatively fine spatial and temporal resolution is critical to understand the overall health of the local population and predict future fish kills. We conducted four surveys during the summer and fall of 2015 after these fish kills using vertical sampling echosounders and sidescan sonar with video and photographic ground truthing. This work was conducted to provide to produce a quantitative estimate of the post-kill menhaden abundance and distribution in the western Peconic Estuary. Furthermore, we demonstrated the application of fishery acoustics methods to assess menhaden and other forage fish in a very shallow water (<2 m) estuarine habitats.

Methods

Four acoustic surveys were conducted in the shallow (< 4 m) waters of Flanders Bay and Peconic River on 19 June, 30 June, 22 July, and 4 November 2015 (Figure 1). In order to estimate total menhaden abundance over the entire Flanders Bay and Peconic River region, the survey track was partitioned into three separate sections accounting for different bathymetric conditions (Kahle and Wickham, 2013): Flanders Bay (from the eastern edge of Flanders Bay to the mouth of the Peconic River), the Lower River (from the river mouth to Rt. 105 bridge), and the Upper River (from Rt. 105 bridge to the western edge of the estuarine portion of the Peconic River). The Flanders Bay, Lower River, and Upper River regions respectively cover 2.62 km^2, 0.17 km^2, and 0.04 km^2 and have respective maximum depths of 4.5, 2.5, and 2.5 m. Cruise tracks were limited to navigable boating channels and survey speeds were approximately 2.3 m/s. Sea state conditions on all four sampling dates were relatively calm with little wind and waves less than 1 ft.

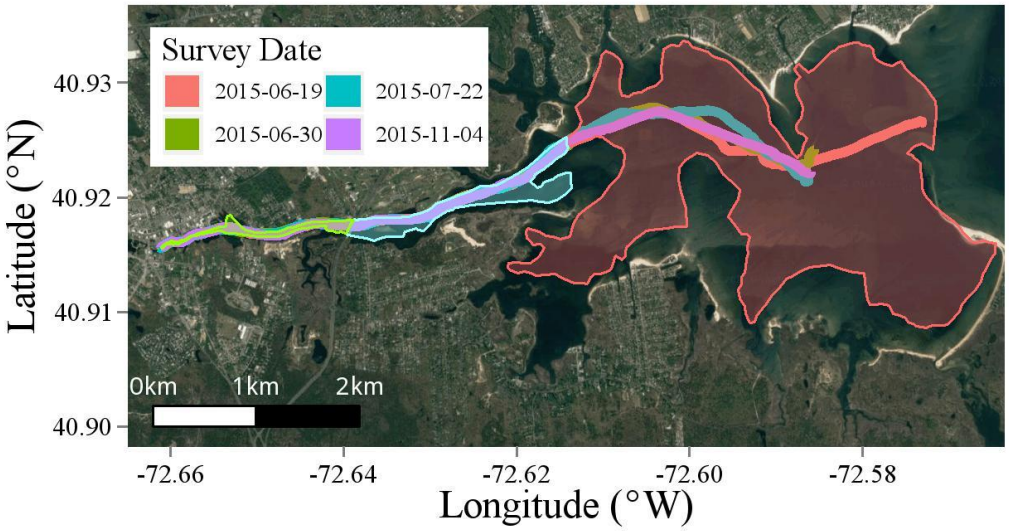

Figure 1. Overview of acoustic survey tracks on 19 June, 30 June, 22 July, and 04 November 2015 (red, green, blue, and magenta respectively) and partitioned regions (light green, blue, and red for the Upper River, Lower River, and Flanders Bay respectively).

Volumetric backscatter (S_v, dB re: m^{-1}) and target strengths (TS, dB re: m^{-2}) were recorded using a 120 kHz split-beam scientific echosounder (Simrad ES60; Table 1). A Humminbird 898c (455 kHz) sidescan sonar was used to collect imagery of fish schools and bottom features. Acoustic transducers were deployed via a pole-mount from the portside of the R/V Steinbítur (Stony Brook University) at an approximate depth of 0.5 meters. Echosounders were calibrated using standard methods (Foote *et al.* 1987) off-shore of Long Island at an approximate depth of 10 m on 10 September 2015 (Foote *et al.* 1987). Physical samples and photography of predation and beach seining were used to ground-truth presence of menhaden (Figure 2). Aggregation parameters were collected from both the sidescan and echosounder data. Spatial measurements (i.e., school width, length-to-width aspect ratios) and GPS coordinates of menhaden schools off-axis of the echosounders were obtained using sidescan data. All TS, S_V, school height and length, GPS location, depth, and time of day were acquired from the echosounder data. It was assumed that all acoustic backscatter and TS measurements came from menhaden and did not include other forage and/or piscivorous predators.

Table 1. Instrument and calibration settings for each transducer.

	38 kHz	**120 kHz**	**200 kHz**
Manufacturer	Simrad	Simrad	Simrad
Beam Pattern	Single-beam	Split-beam	Single-beam
Pulse Length (ms)	0.256	0.256	0.256
Ping Interval (s)	0.500	0.500	0.500
Transmit Power (W)	1000	1000	1000
Half-power Beam Width (Degrees)	15.20	7.00	7.20
Equivalent Beam Width (dB re 1 str)	-14.00	-21.00	-20.50
Transducer Gain (dB)	17.50	27.00	26.30
Absorption Coefficient (dB/m)	0.010	0.038	0.053

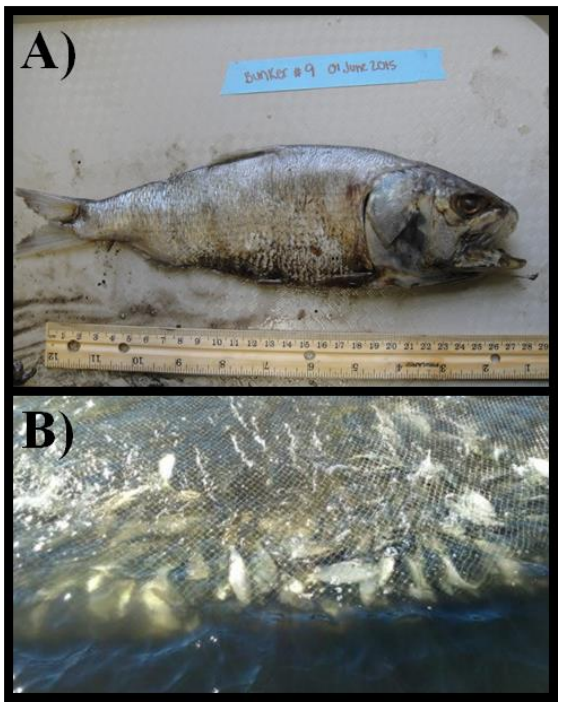

Figure 2. Dead menhaden collected post-kill on 1 June 2015 (**A**) and menhaden caught in a purse seine by local baymen in the Peconic River on 4 November 2015 (**B**).

Acoustic backscatter data were processed and analyzed with Echoview 7.1 (Myriax 2016) and R 3.1.2 (R Core Team 2014). A surface exclusion line was set at a depth of 1.2 m to account for transducer depth, nearfield ranges, and surface noise. A bottom-detection algorithm with a 0.2 m back-step was used remove backscatter that may have comprised both near-bottom aggregations and the seabed. These bottom-lines were visually scrutinized and compared to depths provided by the sidescan sonar Menhaden aggregations were defined using a multifrequency filtering algorithm adapted from Fernandes (2009). A minimum and maximum S_V-threshold of -65 and -15 dB, respectively, was applied

to all three frequencies. A 3x3 median filter was then applied to all echograms and then summed; only totals greater than -150 dB were accepted as menhaden aggregations. The accepted echogram regions were then used to mask over the original 120 kHz S_V echograms. Since only parts of some schools were directly sampled by the echosounders, these accepted regions were then further differentiated into general aggregations and schools using a modified school-detection algorithm (Barange 1994; Fernandes 2009; Figure 3). School-detection parameters were set to the following criteria: minimum total length of 10 m, minimum candidate length of 5 m, maximum horizontal linking distance of 2 m, and a minimum nautical acoustic area scattering coefficient (NASC, $m^2\ nmi^{-2}$) of 500 $m^2\ nmi^{-2}$.

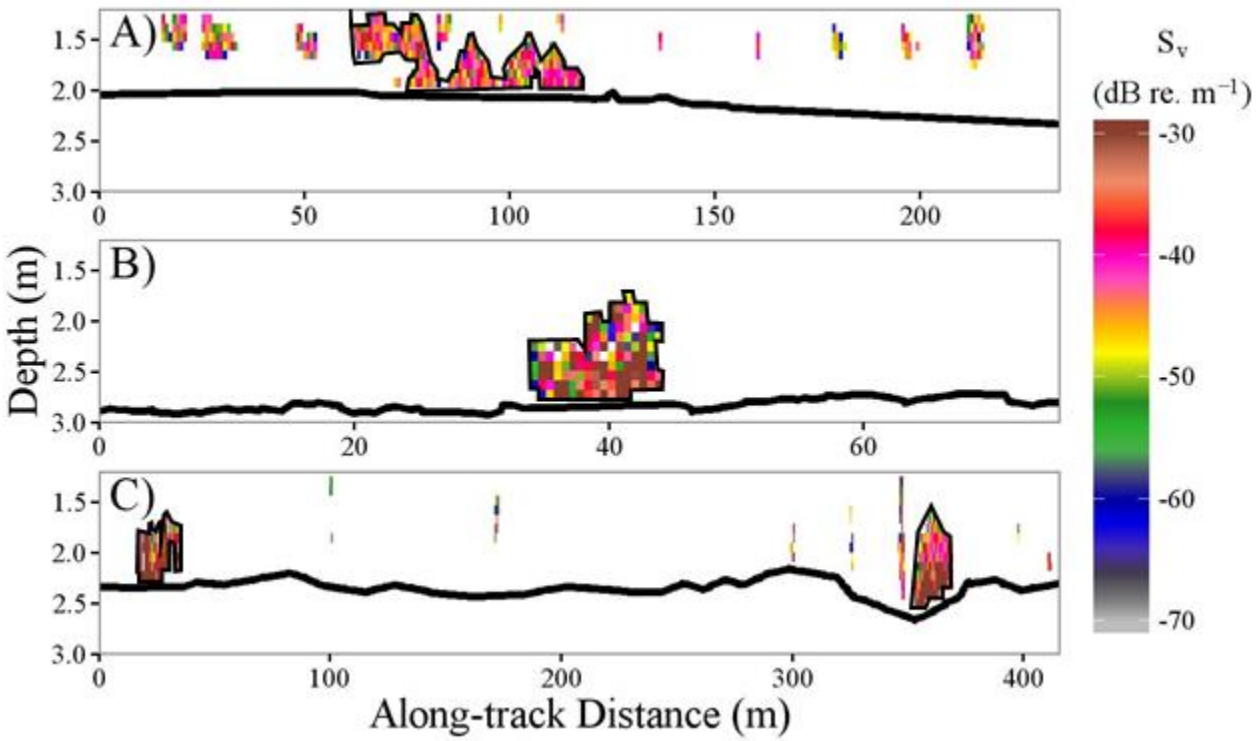

Figure 3. Accepted echogram aggregations and schools at 120 kHz were observed in close proximity (**A**), completely solitary (**B**), and spatially patchy (**C**). Aggregations outlined with a solid black line indicate schools identified via the school-detection algorithm. The thicker solid black line which runs the entire length of each echogram indicates the seabed.

Target strength measurements were made using Echoview's single target detection method (method 2) for split-beam echosounders was applied to accepted aggregations and schools at 120 kHz to filter out multiple targets contributing to a single echo return. For this algorithm, detection parameters were set with the following criteria: minimum and maximum thresholds of -75 and -25 dB respectively, maximum beam compensation of 12 dB, maximum standard deviation of minor- and major-axis angles of 10.0, pulse length determination level of 6 dB, 0.7 to 1.5 minimum to maximum normalized pulse length, and a Simrad LOBE beam compensation model.

School dimensions (i.e., length and width) and geographic locations from sidescan data were processed using Matlab R2014b (The Mathworks 2014). Sidescan acoustic measurements had a maximum athwartship range of 15.0 m due to the shallow depths surveyed on both the port and starboard of the

vessel. Sidescan data provide an additional method for identifying fish aggregations both on- and off-axis of the vertical beam scientific echosounders (Figure 4).

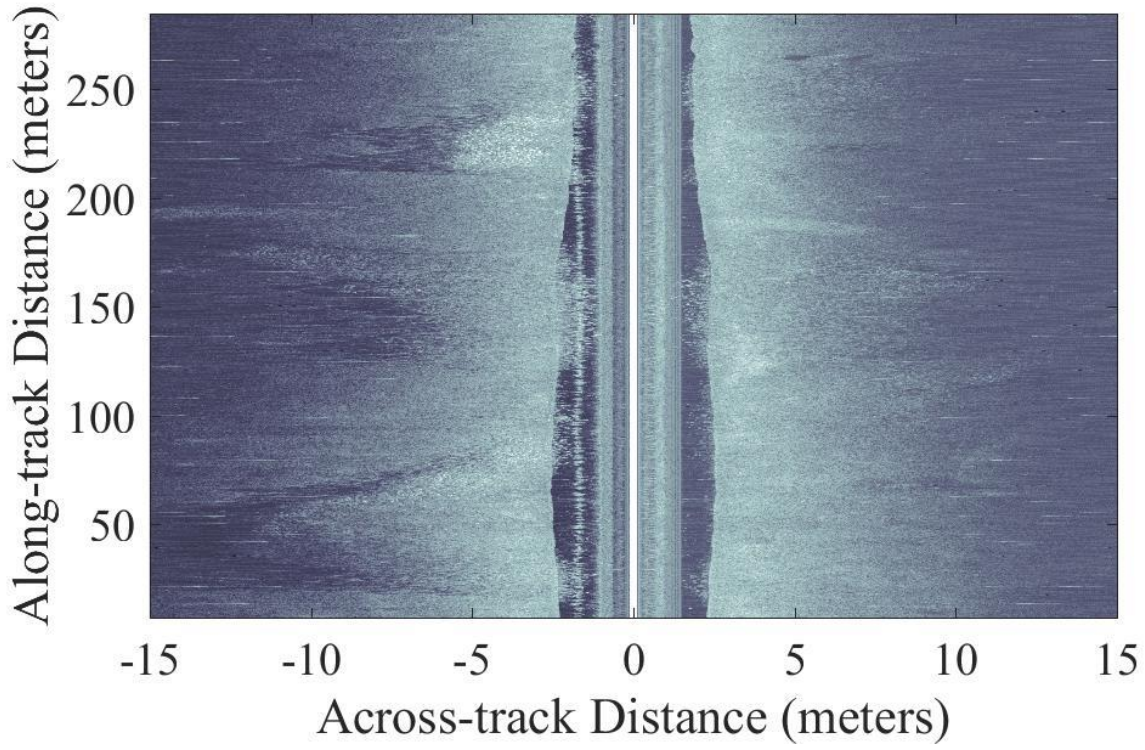

Figure 4. Sidescan image of multiple large menhaden aggregations at along-track distances of approximately 50, 150, and 225m in the Peconic River were observed by the sidescan sonar on 4 November 2015. The dark region in the middle of the image represents the area directly under the vesselsidescan sonar which is only sampled by the vertical beam echosounders.

Abundance and Biomass Estimation

Transects for each survey were broken up into evenly spaced elementary distance sampling units (EDSUs; Simmonds and MacLennan 2006) of 25 m each. Mean EDSU NASC and TS (in the linear domain as σ_{bs} which represents the acoustic scattering cross-section [m^{-2}] of a target) were calculated for each survey region on each date. Mean fish numerical areal density (ρ_A, fish/m^2) was then calculated via $\rho_A = NASC/4\pi\sigma_{bs}(1852)^2$ (Simmonds and MacLennan 2006). The total extrapolated numerical fish abundance for each region on each sampling date was calculated in two parts. First, extrapolated fish abundance for each region was estimated using just the echosounder backscatter data (N_{ei}):

$$N_{ei} = \rho_A A_i \quad (1),$$

where A_i is the total area for each region as shown in Figure (1). Second, Sidescan schools were assigned the mean ρ_A from schools on their respective sampling date. Abundances for each of these

schools were then estimated from the product of their respective ρ_A and area coverage (i.e., the product of their length and width). The extrapolated sidescan abundance (N_{si}) was estimated by:

$$N_{si} = \rho_{AS} A_i \text{ (2)},$$

where ρ_{AS} is defined as

$$\rho_{AS} = \frac{N_{ssi}}{A_i},$$

where N_{ssi} is the summed sidescan abundance for each region. The total extrapolated fish abundance for each region (N_i) was then calculated by the sum of N_{ei} and N_{si}.

In order to estimate biomass, TS measurements were sequentially converted into total length (TL, cm) and then wet weight. First, a TS-length model adapted from Love (1971) was used to estimate the TL:

$$TL = 10^{\left(\frac{TS+63.88-0.9\log_{10}\left(\frac{c}{f}\right)}{19.1}\right)} \text{ (3)},$$

where c and f represent the sound speed in water (cm/s) and frequency (kHz) respectively. Prior to any acoustic sampling, individual dead menhaden were collected from Iron Point beach, Flanders, NY on 1 June 2015 following the 27 May 2015 fish kill in the Peconic River. Fork length (FL, cm) was measured for all encountered fish that were intact length-wise (N = 30) and was compared to acoustic estimates of mean fish length via a linear regression obtained from Smith *et al.* (2008) specific to menhaden:

$$TL_{mm} = 1.15FL_{mm} - 1.65 \text{ (4)},$$

where TL_{mm} and FL_{mm} are the total and fork fish lengths respectively in millimeters. The wet weight (W, g) was then estimated using an empirical weight-length model specific to menhaden (AMSFC 2010):

$$\ln(W) = -11.029TL_{mm}^{3.010} \text{(5)}.$$

Biomass (B, kg) for each region on every sampling date was then calculated by multiplying the mean wet weight (W_{kg}, kg) by total abundance: $B = N_1 W_{kg}$.

Since it was predicted that multiple age and size classes of menhaden would be found in the western Peconic Estuary based on anecdotal observations and studies conducted in other coastal estuaries (Ahrenholz 1991; Rogers and van den Avyle 1983; Smith *et al.* 2008), TS distributions were apportioned into discrete size classes and age classes (Table 2). Size ranges were based on size-at-catch measurements and ages at which significant morphological metamorphosis occurs (Reintjes 1969; SEDAR 2015; Smith *et al.* 2008). Abundance and biomass of each class in each region on every sampling date was estimated via $N_i P_c$ and BP_c respectively where P_c is the relative proportion of each class.

Table 2. Size and TS range for different age classes of menhaden (Reintjes 1969; SEDAR 2015; Smith *et al* 2008).

Age Class	Size Range (cm)	TS Range (dB)
Larvae	2.0 to 3.0	TS < -54.7
Prejuvenile/Juvenile	3.0 to 7.5	-54.7 ≥ TS < -47.1
Young-of-the-year	7.5 to 16	-47.1 ≥ TS < -40.8
Age-1+	16 to 22	-40.8 ≥ TS

Uncertainty Estimation

In order to estimate the overall uncertainty in the abundance and biomass estimates, we attempted to account forquantified known errors by estimating the standard uncertainties for each variable. The 'root sum of squares' (RSS) method (Taylor and Kuyatt 1994) was used to calculate the combined standard uncertainty for abundance and biomass estimates:

$$u(B_{it} \vee N_{it}) = \sqrt{u(NASC_{it})^2 + u(TS_{it})^2 + u(C_{it})^2} \text{ (6)},$$

where terms contained with *u*() represent the coefficient of variation (*CV*) of each term in each region (*i*) on each sampling date (*t*) and *C* is the sampling coverage. A Type A evaluation of uncertainty (Taylor and Kuyatt 1994) was used to estimate the *CV* for NASC and TS:

$$u(TS_{it} \vee NASC_{it}) = \frac{SE}{\bar{x}} \text{ (7)},$$

where SE and *x* represent the standard error and mean of each term respectively. Methods from Aglen (1989) were used to estimate sampling coverage error:

$$u(C_{it}) = \frac{0.5}{\sqrt{(\frac{D_{it}}{\sqrt{(A_i)}})}} \text{ (8)},$$

where D_{it} is the cruise track length in each region on each sampling date.

Statistical Analysis

Variography was used to test for any spatial structure in EDSU NASC on each sampling date using a spherical semivariogram model (Cressie 1993). For each empirical variogram a lag distance of 50 m was used and NASC was transformed via $\log_{10}$(NASC + 0.1). Great-circle distances between EDSUs were estimated based on the coordinates (i.e., longitude, latitude) at the middle of each segment. A type-II analysis of variance (ANOVA, $\alpha = 0.05$) was conducted to detect differences in mean EDSU NASC and TS among regions and sampling dates. *Post hoc* pairwise comparisons were done using a Tukey's Honest Significance test (Tukey HSD, $\alpha = 0.05$). Pairwise comparisons of transect directions were done using a Welch Two Sample *t*-test (*t*-test, $\alpha = 0.05$).

Results

Significant differences in mean EDSU NASC were detected among regions (ANOVA, $F_{(2,1941)} = 11.96$, $p < 0.01$), among regions on each sampling date ($F_{(6,1941)} = 2.49$, $p = 0.02$), but not overall among sampling dates ($F_{(3,1941)} = 1.99$, $p = 0.11$). Among all sampling dates mean NASC in the Upper River (840 m^2nmi^{-2}, $N = 527$, $CV = 0.28$) was significantly higher (Tukey HSD, $p < 0.01$) than both the Lower River (130 m^2nmi^{-2}, $N = 488$, $CV = 0.21$) and Flanders Bay (140 m^2nmi^{-2}, $N = 938$, $CV = 0.11$). There was no significant difference in mean NASC between Flanders Bay and the Lower River ($p = 0.99$). This regional trend whereby peak NASC values were observed in the Upper River was only absent during 22 July (Figure 5). NASC during this survey ranged from 10 to 120 m^2nmi^{-2} between the Upper River and Flanders Bay respectively; however, was there were no significant differences in mean NASC between any of the regions ($p = 1.00$). Likewise, CV estimates for the Upper River (1.00), Lower River (1.00), and Flanders Bay (0.32) reflected the high variability between EDSUs containing empty water and the sudden appearance of schools with relatively high NASC (9,100 m^2nmi^{-2}, $N = 2$, $CV = 0.43$). Comparatively while there were no significant differences in mean NASC among sampling dates (ANOVA, $F_{(3,33)} = 0.64$, $p = 0.59$) there were significantly fewer schools on 22 July than on 19 June (11,000 m^2nmi^{-2}, $N = 9$, $CV = 0.58$), 30 June (10,400 m^2nmi^{-2}, $N = 9$, $CV = 0.57$), and 04 November (4,500 m^2nmi^{-2}, $N = 17$, $CV = 0.28$).

Another notable trend were the differences between the westward and eastward transects. Mean NASC measured along westward transects (520 m^2nmi^{-2}, $N = 1{,}095$, $CV = 0.22$) were significantly higher (t-test, $t = 2.83$, $p < 0.01$) than their respective eastward tracks (80 m^2nmi^{-2}, $N = 858$, $CV = 0.12$) by almost a full order of magnitude. This result was also reflected significantly higher number and mean NASC of schools along westward (8,500 m^2nmi^{-2}, $N = 33$, $CV = 0.28$) transects compared to eastward transects (1,400 m^2nmi^{-2}, $N = 4$, $CV = 0.44$; $t = 0.285$, $p = 0.01$). The significant differences in number of schools between westward (8, 7, 2, and 16) and eastward transects (1, 2, 0, and 1) on 19 June, 30 June, 22 July, and 04 November respectively change slightly when incorporating schools identified via sidescan sonar detection.

A total of 35 aggregations were identified via sidescan sonar with along- and across-tracks ranging from 4 to 30 and 3 to 13 m respectively. There were no detections along either transect on 22 July. Roughly half of these aggregations ($N = 18$) qualified as schools based on their respective lengths (i.e., at least 10 m). The proportion of schools compared to the total number of aggregations among sampling dates (4 of 6, 0 of 4, and 14 of 25 for 19 June, 30 June, and 04 November respectively) resembled those detected by the echosounders whereby the peak number of schools occurred on 04 November. However, differences in the number of schools along eastward (2 and 8) and westward (2 and 6) on 19 June and 04 November differed from the trend observed in both EDSU NASC and echosounder school occurrence. Likewise, there was no significant difference (t-test, $t = -1.10$, $p = 0.29$) in mean school lengths along westward (15 m, $N = 8$, $CV = 0.08$) and eastward (18 m, $N = 10$, $CV = 0.10$) transects. Although the acoustic density (i.e., NASC) of sidescan schools could not be directly measured, there was no significant difference in mean length of echosounder (20 m, $N = 37$, $CV = 0.09$) and sidescan schools (17 m, $N = 18$, $CV = 0.07$; t-test, $t = 1.71$, $p = 0.09$). With echosounder and sidescan schools combined, 36, 20, and 16 schools were observed in the Upper River, Lower River, and Flanders Bay respectively.

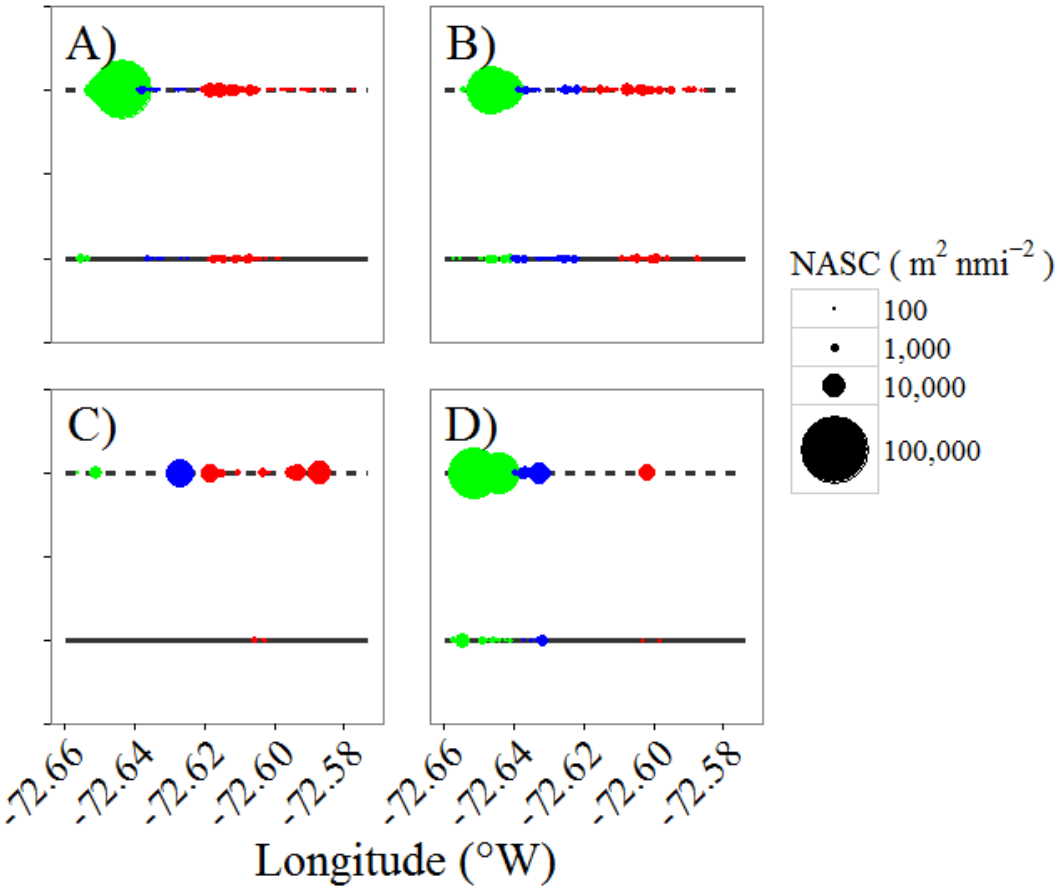

Figure 5. Distribution of EDSU NASC for each westward (dashed line) and eastward (solid line) transects on 19 June (**A**), 30 June (**B**), 22 July (**C**), and 04 November (**D**). The areas of each point is scaled to its respective NASC value. Green, blue, and red colored points represent those in the Upper River, Lower River, and Flanders Bay respectively.

There was also significant spatial structure across all survey dates (Figure 6). The nugget effect accounted for 48%, 80%, 69%, and 92% of the variance of EDSU NASC on 19 June, 30 June, 22 July, and 04 November respectively. This would indicate relatively low spatial structure in all but the 19 June sampling date. The partial sill and range on 19 June (1.90 and 0.58 respectively) were higher than the other three sampling dates which suggests that spatial variance and structure decreased after 19 June. Comparatively, the relatively low partial sill and range on 22 July (0.26 and 0.26 respectively) reflects the relatively high variability in mean EDSU NASC observed among regions and a consequence of few schools and large aggregations.

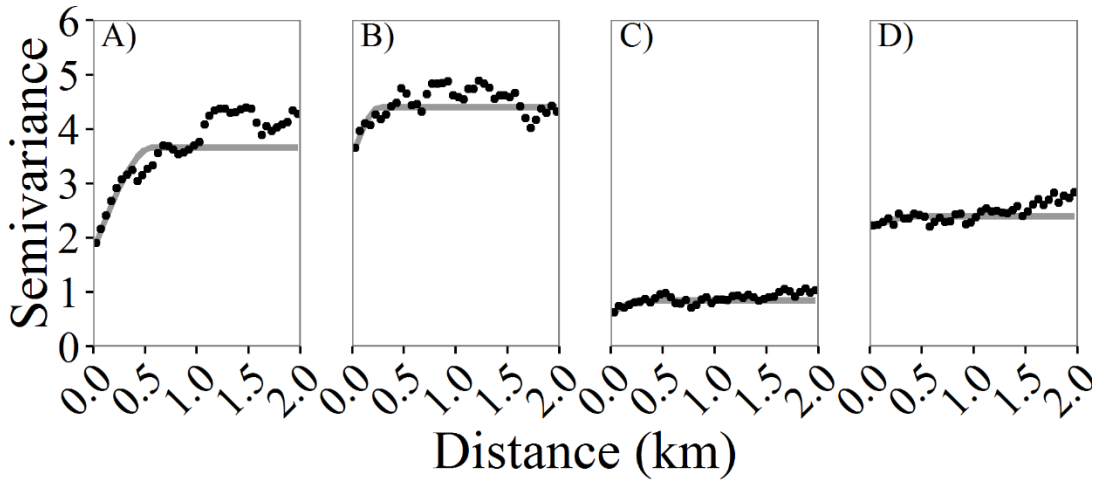

Figure 6. Semivariograms of EDSU NASC values on 19 June (**A**), 30 June (**B**), 22 July (**C**), and 04 November (**D**). Lag interval used was 50 meters with 40 total lags. Black points represent the empirical variogram. The gray line represents the fitted spherical-model variogram.

Target Strength

There were significant differences detected in mean TS among sampling dates (ANOVA, $F_{(6,1067)} = 29.07$, $p < 0.01$), regions ($F_{(6,1067)} = 85.56$, $p < 0.01$), and among regions across all sampling dates ($F_{(6,1067)} = 20.78$, $p < 0.01$). Mean TS on 04 November (-40.8 dB, $N = 166$, $CV = 0.17$) was significantly higher than on 19 June (-45.8 dB, $N = 587$, $CV = 0.24$; Tukey HSD, $p < 0.01$), 30 June (-46.2 dB, $N = 253$, $CV = 0.17$; $p < 0.01$), and 22 July (-49.4 dB, $N = 73$, $CV = 0.15$; $p < 0.01$). Moreover, all pairwise comparisons among sampling dates were significantly different ($p < 0.03$). This seasonal increase was also reflected in the frequency distribution shapes for each region (Figure 7) When converted to TL using equation (3) these TS values correspond to lengths of 9, 8, 6, and 16 cm respectively. Total lengths measured from physical samples collected on 1 June of whole fish ranged from 23.8 to 28.0 cm with a mean of 26.2 cm ($N = 30$, $CV = 0.01$) which corresponds to a TS of -36.7 dB and a range of -37.5 to -36.2 dB.

There was a general decrease in mean TS from the Upper River to Flanders Bays: mean TS in the Upper River (-39.3 dB, $CV = 0.14$) was significantly higher than in the Lower River (-51.3 dB, $CV = 0.28$; Tukey HSD, $p < 0.01$) and Flanders Bay (-54.1 dB, $CV = 0.26$; $p < 0.01$). There was no significant difference between the Lower River and Flanders Bay. This regional trend held true among all sampling dates except for 22 July which was likely a consequence of the presence of few schools and large aggregations. Once partitioned into the TS-defined size classes from Table (2), there were also significant differences among sampling dates ($\chi^2(9) = 271.7$, $p < 0.01$), regions ($\chi^2(6) = 1101.4$, $p < 0.01$), and among regions on each sampling date ($\chi^2(9) = 591.2$, $p < 0.01$). The larvae, pre-juvenile/juvenile, young-of-the-year, and adult size classes comprised 66%, 23%, 6%, and 5% of all single targets, respectively.

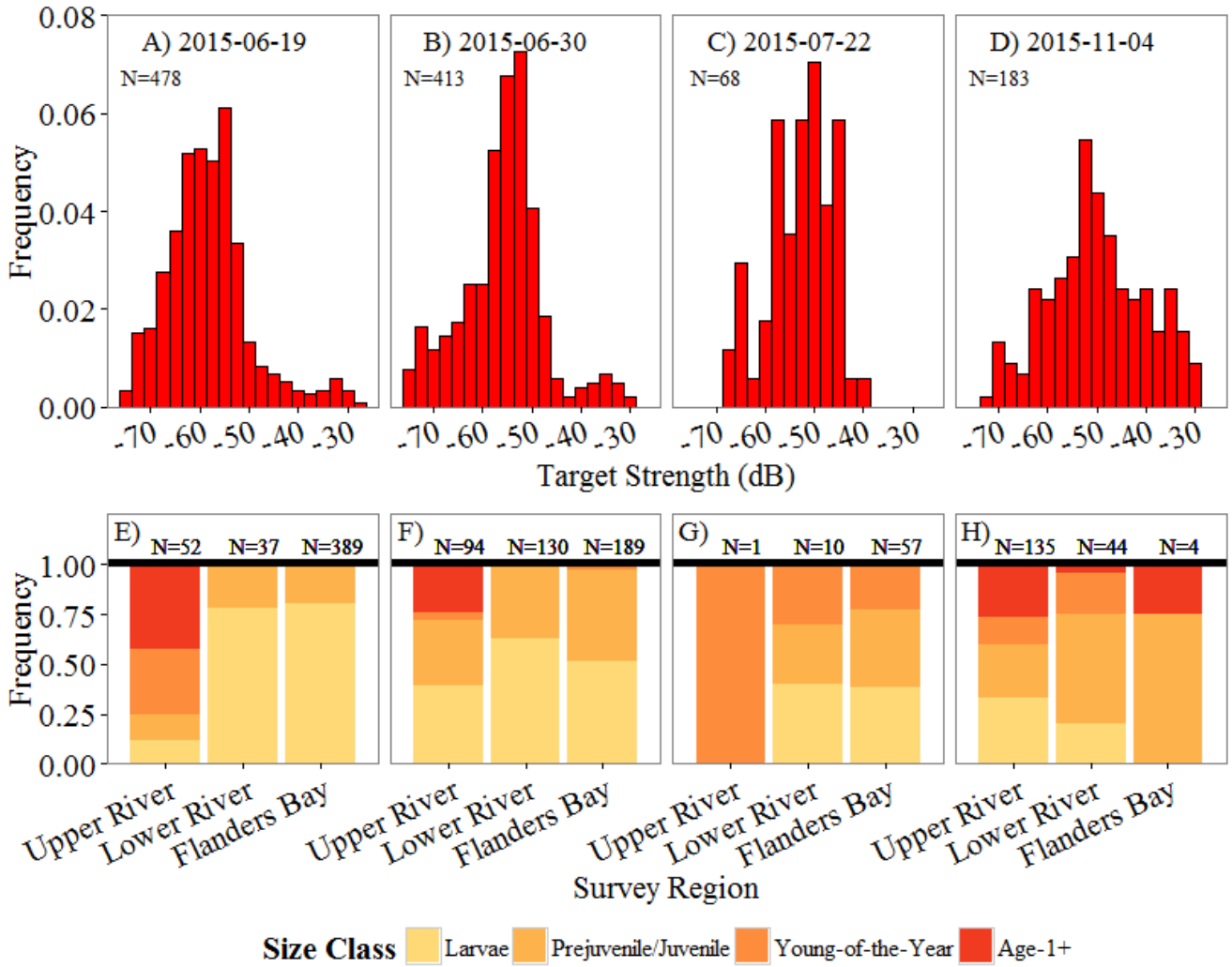

Figure 7. Frequency distribution of single target TS for 19 June (**A**), 30 June (**B**), 22 July (**C**), and 04 November (**D**). The TS-derived size-class compositions for each date and region were broken up for each sampling date (**E-H** respectively).

Abundance and Biomass Extrapolation

Extrapolated abundance estimates varied by almost three orders of magnitude between survey regions and one order of magnitude between survey dates (Table 3). Estimates of total abundance and areal fish densities (fish/m^2) peaked on 19 June (5,347,000 fish, 1.89 fish/m^2) and was significantly higher than 30 June (2,061,000 fish, 0.72 fish/m^2), 22 July (496,000 fish, 0.18 fish/m^2), and 04 November (102,000 fish, 0.04 fish/m^2). In the context of the 2015 Peconic fish kill, the SCDHS estimate of approximately 250,000 represented between. In the context of the 2015 Peconic fish kill, the SCDHS estimate represented between 3-8% of our abundance estimate immediately after the fish kill (19 June). Regional differences in abundance among all sampling dates resulted in the lowest abundance estimates in the Upper River which increased to their apex in Flanders Bay. In terms of areal fish density, aside from 22 July the Upper River had the highest fish/m^2 on 19 June (8.8 fish/m^2), 30 June (4.3 fish/m^2), and 04 November (0.7 fish/m^2) compared to the Lower River (0.2 fish/m^2, 0.8 fish/m^2,

0.12 fish/m^2 respectively) and Flanders Bay (1.9 fish/m^2, 0.7 fish/m^2, and 0.1 fish/m^2) on the same sampling dates.
Extrapolated biomass ranged (excluding the values < 100 kg in the Upper and Lower River on 22 July) from approximately 400 to 55,900 kg with areal biomass densities between 600 and 99,300 kg/km^2. Similar to the abundance estimates, aside from 22 July areal biomass densities (kg/km^2) were highest in the Upper River on 19 June (99,300 kg/km^2), 30 June (41,800 kg/km^2), and 04 November (49,600 kg/km^2) compared to the Lower River (2,300, 7,600, and 8,700 kg/km^2 respectively) and Flanders Bay (21,300, 6,600, and 1,400 kg/km^2 respectively) on the same sampling dates.

Table 3. Extrapolated estimates of abundance (1000s fish), biomass (kg), and combined standard uncertainty for the Upper River, Lower River, and Flanders Bay on 19 June, 30 June, 22 July, and 04 November 2015.

	Upper River			**Lower River**			**Flanders Bay**		
Sampling Date	N_i (1000s fish)	B_i (kg)	*CSU* (%)	N_i (1000s fish)	B_i (kg)	*CSU* (%)	N_i (1000s fish)	B_i (kg)	*CSU* (%)
19 Jun.	337	3,800	73.4	38	400	48.7	4,972	55,900	44.5
30 Jun.	163	1,600	59.8	131	1,300	37.1	1,767	17,300	44.5
22 Jul.	<1	< 100	102.4	14	< 100	104.7	481	1,500	54.3
04 Nov.	27	1,900	42.6	22	1,500	46.9	53	3,700	93.6

Uncertainty Estimates

Standard uncertainties for EDSU NASC among regions on each sampling date ranged from 14.9 to 100% (86.4% excluding the errors from the Upper, 99.9%, and Lower, 100.0%). Error in TS ranged from 14.5 to 22.8%. Sampling coverage error ranged from 17.0 to 36.8%. Overall, the combined standard uncertainty for each sampling region on each survey date ranged from 37.1 to 104.7%.

DISCUSSION

Abundance and Biomass Estimates

The estimated number of menhaden killed during the 2015 fish kills represented 3-8% of our abundance estimates for the western Peconic Estuary in the immediate aftermath (19 June). A seasonal trend can be inferred between the late spring, early summer that immediately followed the fish kills (19 and 30 June), mid-summer (22 July), and late fall (04 November). Despite very high uncertainty during the 22 July survey (Upper and Lower River) due to the patchiness and variability in presence of schools, the total number and numeric areal density of fish monotonically decreased across all surveys by two orders of magnitude. There was a similar trend, albeit non-monotonic, observed in biomass estimates. Biomass was heavily concentrated in EDSUs that contained schools and contributed to high areal biomass densities (kg/m^2) in the Upper and Lower River despite being an order of magnitude lower than Flanders Bay in total biomass. This is reflected in the spatial distribution of mean EDSU NASC on each sampling date (Figure 5) and the relatively small lags in their respective variograms (Figure 6). It also is likely the result of a decreased sampling volume due to shallower depths and smaller area coverage of water (e.g., the Upper River versus Flanders Bay). For instance, the theoretical

maximum packing density (fish/m^3) of schooling fish can be approximated from the relation $(2L)^{-3}$ where L is the length of an individual fish in meters (Misund 1993; Pitcher and Partridge 1979).

Since temporal trends in TS can be used as a general proxy measurement for changes in age/size class over time (Simmonds and MacLennan 2006), the observed increase from spring to fall (-49.4 to -40.8 dB) represents an approximate tripling in size class (i.e., 6 to 16 cm; Figure 7A-D). In terms of school packing density this would represent a range of 30 to 580 fish/m^3. Consequently, despite the presence of more schools on 04 November, abundance estimates were highest in 19 and 30 June due to their respective lower mean TS values. Conversely, despite having significantly less fish than on 30 June in the Upper and Lower River, fish biomass on 04 November in these regions were higher due to the significantly higher mean TS. However, the gradual change in TS distribution over time resembles length-frequency distributions of menhaden over both short (i.e., days) and long (i.e., weeks to months) periods of time (Ahrenholz *et al.* 1989). Therefore, these trends in abundance and biomass were a function of TS and changes in TS-defined age classes.

The frequency of larvae decreased among surveys with concomitant increases in young-of-the-year and age-1+ fish (Figure 7E-H). This trend is consistent with seasonal behaviors of menhaden in other North Atlantic coastal estuaries where adults and young-of-the-year begin migrating offshore and southward towards North Carolina by early- to mid-fall (Ahrenholz 1991). It may also reflect the relative growth of age-0 menhaden within estuaries and continued spawning throughout the summer in favorable conditions (Reintjes 1969; Rogers and van den Avyle 1983). According to the most recent stock assessment of menhaden, age-0 and age-1+ fish make up 51 and 49% of the entire population respectively (SEDAR 2015). Contrarily, our TS-derived distributions were heavily dominated by age-0 fish (~91%); however, this discrepancy can be explained due to sampling effort being limited to the shallow water estuary where younger, smaller fish are more likely to be encountered.

The ecological implications of a population dominated by age-0 population has several important ecological implications. First, since size and age distributions of adult menhaden are linked to relative recruitment success of coastal estuaries (Quinlan *et al.* 1999; SEDAR 2015), it stands to reason that recruitment success and fecundity of local menhaden populations can be qualitatively inferred from age-0 dominated populations. Age-0 menhaden have been observed to be an important prey item for smaller, younger bluefish and striped bass (Hartman and Brandt 1995). In extension, as age-0 menhaden successfully develop and survive, their emigration from the very shallow waters of estuaries results in increased prey availability for other pelagic predators limited to relatively deeper waters such as bluefin tuna (Butler *et al.* 2010) and humpback whales (Ahrenholz 1991). Conversely, one ecological consequence (alongside economic damages) of increased menhaden abundance is more frequent fish kills (O'Shea and Brosnan 2000); however, these kills can provide a large food source for scavengers such as benthic crustaceans and seabirds. Some comparisons can be made between the western Peconic Estuary and Chesapeake Bay where hypoxic/anoxic events (< 3 mg/L) became, or are becoming, more frequent. Major perturbations in menhaden populations alongside other biological stresses such as disease, harmful algal blooms, water contamination, and fishing pressure, similar losses in suspension-feeding shellfish, and other factors can have extreme negative consequences on piscivorous fish that rely on menhaden as a key prey item (Jackson *et al.* 2001; Uphoff 2003).

Target Identification and Accuracy

Although other forage fish species such as Atlantic silversides and alewives are also observed in the Peconic Estuary (Bortman and Niedowski 1998), they are not generally associated with menhaden aggregations in space or time. During the summer, adult Atlantic silversides are generally found spawning in shallower eelgrass beds which are not abundant in the western Peconic. Adult alewives migrate up the Peconic River into fresher waters during the early spring and return in the late fall when juveniles will overwinter in the shallow waters of the western estuary. Due to a lack of trawl data from the western Peconic Estuary throughout the year there remains possibility that some backscatter of identified menhaden schools may be from other forage fish. However, the timing of the surveys relative to the ecological behavior of non-menhaden forage fish suggests that the majority of our backscatter data came from menhaden. Menhaden aggregations are also commonly associated with predators such as bluefish and striped bass whose backscatter could not necessarily be ruled out and may comprise a small proportion of larger measured TS values (> -35 dB) but are not generally associated with large, dense schools in shallow waters.

Despite attempts to account for as much uncertainty in our TS distributions as possible, some sources of error remain when measuring *in situ* TS. Expected issues such as multiple scattering from dense aggregations, proximity to the seabed, smaller sampling volume due to a relatively narrow beam width, three-dimensional orientation of fish (i.e., roll, pitch, and yaw), and general morphology and physiology can have a major effect on TS (Simmonds and MacLennan 2006). Without *ex situ* TS experiments or pre-existing acoustic measurements specific to menhaden, our use of Equation (1) may not adequately represent *in situ* TS measurements of menhaden. For instance, menhaden have relatively deeper bodies (i.e., body depth) and angled swim bladders (~18º from the body's mid-line) compared to some other clupeoids whose TS-length relationships have been previously studied (Blaxter and Batty 1990). Future work needs to be done in providing an empirical TS model for menhaden using a combination of *ex situ* modeling and *in situ* ground-truthing.

Conclusion

As Atlantic menhaden populations have increased along the eastern coastal United States (SEDAR 2015), it is important to know the spatial and temporal distributions of these fish, how they impact local ecosystems, and whether or not the population will continue to increase and continue to expand its northward geographic range. It is also important to have baseline knowledge of abundance and biomass in order to infer what effect large disturbances such as the 2015 fish kill have on local populations but also try to predict This work serves as a case study demonstrating that vertically-oriented beam acoustic surveys can provide a quantitative stock assessment of a forage fish in a shallow water estuary. Regular acoustic surveys of forage fish populations in shallow water estuaries can be done rapidly, efficiently, and provide broader spatial coverage than traditional sampling methods.

Chapter 2

Quantification of forage fish (Atlantic menhaden) distribution, abundance, and biomass in the coastal waters of Long Island, New York using acoustic methods.

Introduction

Atlantic menhaden (*Brevoortia tyrannus* Latrobe 1802) is an estuarine-dependent planktivorous fish that is abundant along the entire eastern coast of the United States, particularly from North Carolina to Massachusetts (Ahrenholz 1991). During late spring and early summer, sexually mature adults make annual coastal north-south migrations away from Chesapeake Bay with larger individuals moving further than their smaller counterparts (Nicholson 1978. These migrating adults spawn in various bays and sounds until mid-fall with their eggs and larvae moving into coastal estuaries and wetlands via diel vertical migration and coastal advection (Reintjes 1969; Rice *et al.* 1999). After a rapid metamorphosis from larvae into juveniles, these menhaden either return to coastal waters and join spawning adults as they migrate back towards Chesapeake Bay in the late fall or may overwinter in their respective nursery habitat (Ahrenholz 1991; Reintjes 1969). These juveniles, young-of-year, and adults will aggregate into dense schools that can span hundreds of meters across and can be found in both shallow estuarine and relatively deep coastal waters (Ahrenholz 1991).

As a forage fish that trophically links primary producers and predators, menhaden are an important prey item for many piscivores such as striped bass (*Morone saxatalis*), bluefish, (*Pomatomus saltarix*), and weakfish (*Cynoscion regali)*, seabirds, sharks, and marine mammals such as humpback whales (Ahrenholz 1991). However, many of these predators are in varying states of decline and the rapid decline of other forage fish (Essington *et al.* 2015) and habitat quality of North Atlantic estuaries (Jackson *et al.* 2001) threaten to exacerbate these trends. Although many fisheries have adopted an ecosystem-based fishery management (EBFM) approach to remediate some of these struggling stocks, many have not adequately considered predator-prey interactions primarily due to limited quantitative data (Skern-Mauritezen *et al*. 2015). Consequently, the national menhaden stock is highly susceptible to local disturbances, such as fish kills, during larval/juvenile development and coastal migrations (McHugh 1972; SEDAR 2015) that may indirectly impact the stocks of their predators (Ahrenholz 1991).

Comprehensive menhaden stock assessments generated by the Atlantic States Marine Fisheries Commission (ASMFC) primarily use fishery landings, port samples, and daily logbooks from regional fisheries to generate models that estimate abundance, fishing mortality, biomass, fecundity, and other proxies that represent stock status (SEDAR 2015). Although some fishery-independent data have been incorporated into the most recent assessment models, many regions, such as the coastal and estuarine waters around New York, still lack fishery-independent and trawl data with broad spatial coverage specific to menhaden (SEDAR 2015; Vaughan 2002). As such, there is an increased need for more efficient stock assessment techniques that can adequately estimate menhaden abundance with large spatial and seasonal resolutions abundance in understudied regions, such as off the southern coast of Long Island.

Although acoustic surveys have not been previously used to measure Atlantic menhaden, they have been used to study forage fish such as Gulf menhaden (Boswell *et al.* 2010), sardine (Demer *et al.*

2013), herring (Overholtz *et al.* 2006), and other pelagic coastal fish species (Shen *et al.* 2008). Hydroacoustics is an important tool for effective fisheries management that is time-efficient and provides data with finer resolution in space and time when compared to some traditional sampling methods such as net trawling (Simmonds 2003; Simmonds and MacLennan, 2006; Trenkel *et al*. 2011). Moreover, acoustics is often regarded as an important component for successful EBFM strategies (Handegard *et al.* 2012; Trenkel *et al.* 2011). Likewise, acoustic surveys provide a relatively non-invasive approach that can remotely observe schooling characteristics, physiology, morphology, and life history characteristics (Simmonds and MacLennan 2006).

Nautical acoustic area scattering coefficient (NASC, m^2 nmi^{-2}), which represents the vertically integrated acoustic backscatter integrated over a square nautical mile, is often used as a proxy measurement of numeric fish density or biomass (Simmonds and MacLennan 2006). Target strength (TS, dB re: 1 m^2) is another acoustic measurement that has been used as a proxy index (Trenkel *et* al. 2011) for changes in population size class composition since TS is, in many cases, a function of fish size (Love 1971; Simmonds and MacLennan 2006).

Better estimates of menhaden abundance and biomass in along the coast of southern Long Island is crucial for managing both the species and its predators. We conducted surveys during the summers of 2014 and 2015 at two offshore (~ 6 km) sites using echosounders and sidescan sonar to study schools of menhaden. This study provided a quantitative estimate of menhaden abundance and biomass at these two sites and demonstrated the application of fishery acoustics methods to assess menhaden in pelagic habitats.

Methods

Survey Design

Twenty-six acoustic surveys were conducted at two offshore sites of Long Island at approximately 40°31.884' N -73°43.445' W (Atlantic Beach) and 40°31.250' N -73°32.595 (Hempstead) (Figure 1). Both survey sites had average depths of approximately 20 meters and comprised areas of 1.67 and 3.01 km^2 respectively. Surveys were conducted on 15-18 August 2014, 16-17 April 2015, 19-20 May 2015, 12 and 16 June 2015, 13-14 July 2015, 12-13 August 2015, and 9 September 2015. The survey vessel ran multiple roughly parallel transect lines that varied in length at each site. The heading of transects were reversed depending on wind direction and if sea state became unfavorable (i.e., waves exceeding 1 m).

Hydroacoustic observations were recorded using three Simrad ES60 (38, 120, and 200 kHz) (Table 1). Transducers were mounted on a tow-body deployed at an approximate depth of 0.5 meters off the starboard stern of the R/V Paumanok (Stony Brook University) and towed at an approximate speed of 5 knots. Echosounders were calibrated using a 38.1 mm tungsten carbide sphere at an approximate depth of 10.5 meters on September 2015 (Foote *et al.* 1987). Hydrographic profiles of the water column were measured at each site on each sampling date from vertical CTD (Seabird 19+) casts.

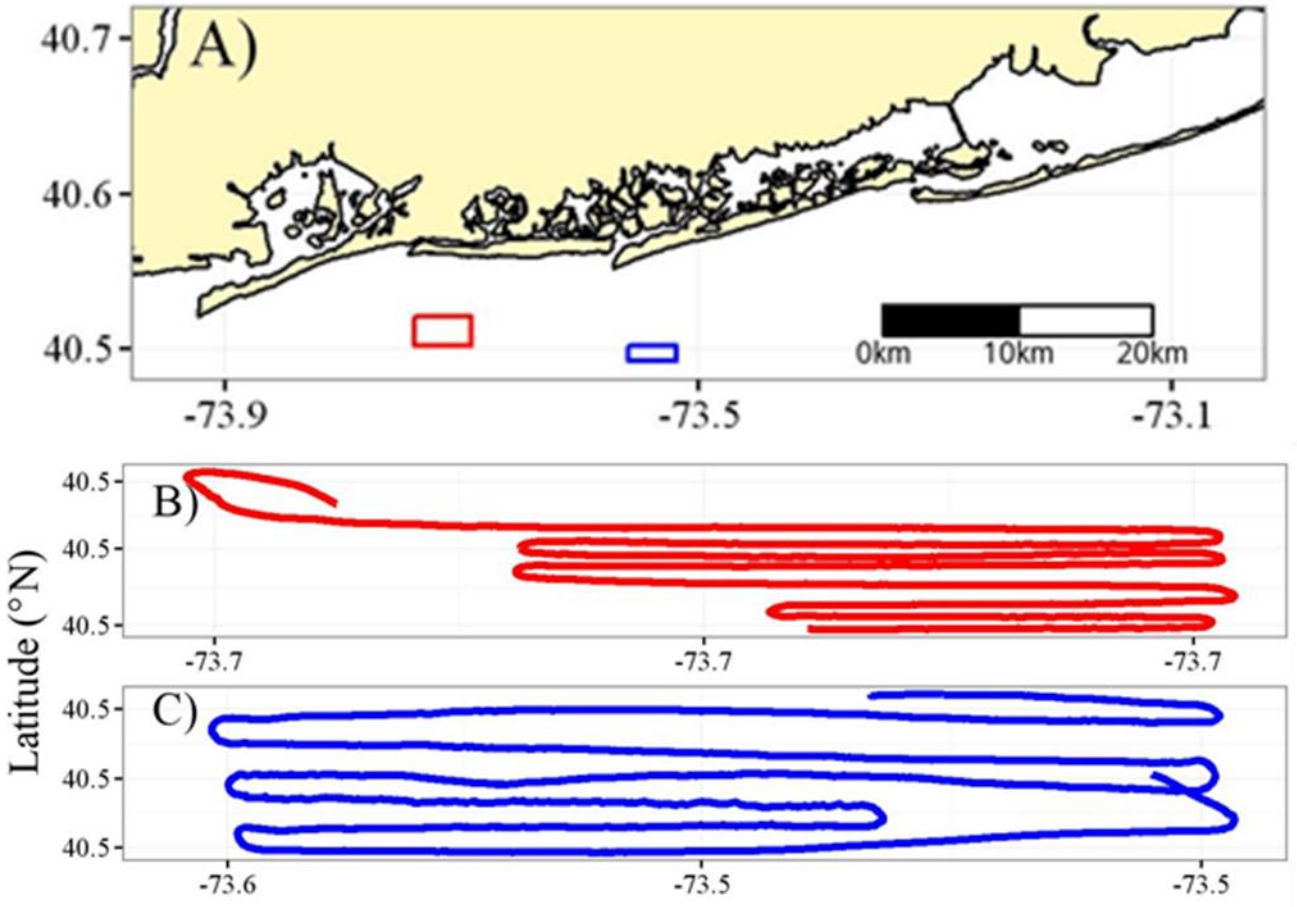

Figure 1. Acoustic surveys were conducted off the southern coast of Long Island (**A**) with semi-parallel transects at two sites: Atlantic Beach (**B**) and Hempstead (**C**).

Table 1. Instrument and calibration settings for each transducer.

	38 kHz	**120 kHz**	**200 kHz**
Manufacturer	Simrad	Simrad	Simrad
Beam Pattern	Single-beam	Split-beam	Single-beam
Pulse Length (ms)	0.256	0.256	0.256
Ping Interval (s)	0.500	0.500	0.500
Transmit Power (W)	1000	1000	1000
Half-power Beam Width (Degrees)	15.20	7.00	7.20
Equivalent Beam Width (dB re 1 str)	-14.00	-21.00	-20.50
Transducer Gain (dB)	17.50	27.00	26.30
Absorption Coefficient (dB/m)	0.010	0.038	0.053

Data Analysis

All hydroacoustic data were processed using Echoview 7.1 (Myriax 2016) and R 3.3.1 (R Core Team 2016). A surface exclusion line set was at 1.5 meters to account for the near-field and surface noise (i.e., bubble intrusion). Acoustic backscatter data from the 120 kHz echograms were used to calculate

mean volume backscattering strength (S_V, dB re m^{-1}), TS, and NASC. Background noise was filtered out based on signal-to-noise ratios based on recommendations by Robertis and Higginbottom (2007). A 3x3 median filter was applied to all three frequencies to remove intermittent background noise. Once smoothed minimum S_V-thresholds were set at -60, -70, and -70 dB at 38, 120, and 200 kHz respectively.

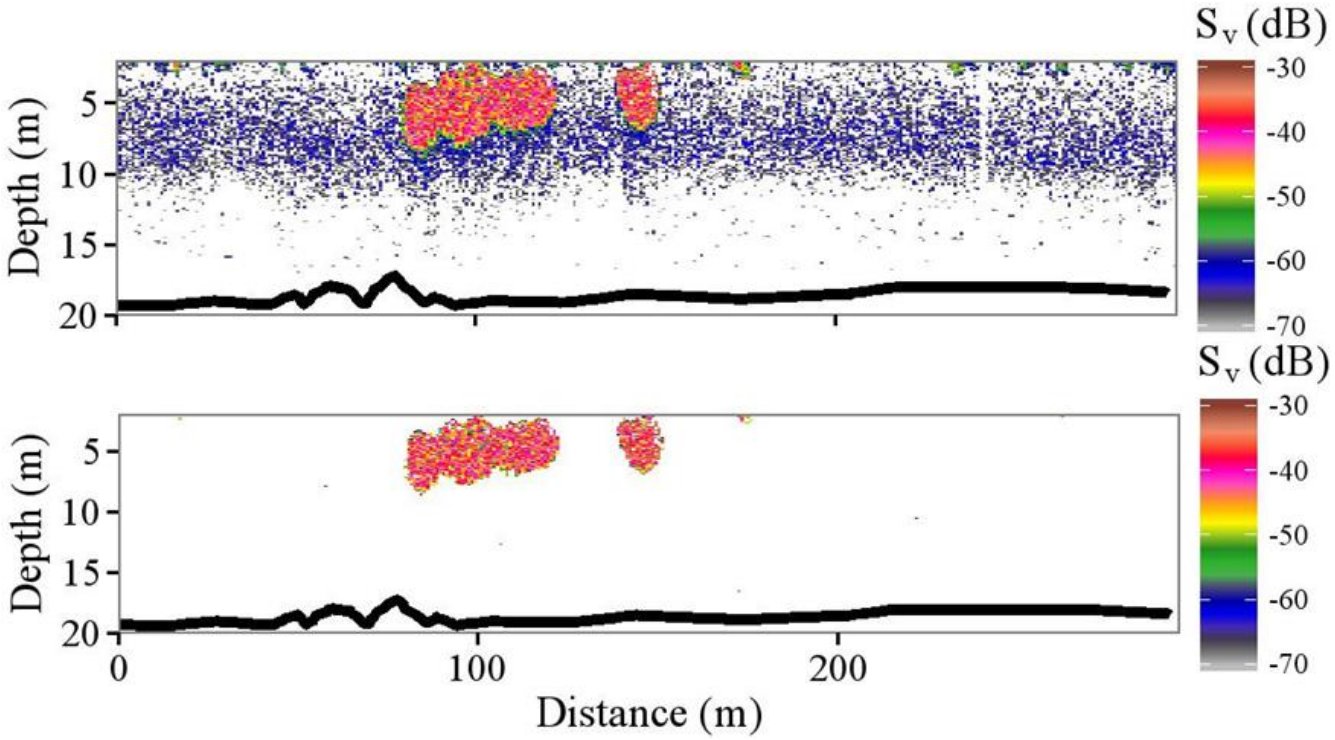

Figure 2. Echograms shown are at 120 kHz before (upper) and after (lower) applying the filtering algorithm. The black lines within represent the sea bottom. The top and bottom images represent the pre- and post-filter echograms respectively. Minimum S_V-thresholds were set for the 38, 120, and 200 kHz echograms (-60, -70, and -70 dB); S_V at 120 kHz was masked where $S_V \forall (S_{V(38+120+200)} > -200)$.

Menhaden schools were defined using an algorithm adapted from Fernandes *et al.* (2009) and then visually inspected to remove non-menhaden aggregations (Figure 2). After thresholding, ping times for all three frequencies were matched to account for the distance between where the echosounders were placed on the towfish. Several methods to account for acoustic shadowing by estimating the extinction cross-section (σ_e) and correction factor were adapted from experiments on herring (Foote *et al.* 1992; Sigler and Scepp 2007). The smoothed S_V from all three frequencies were summed and all values less than -100 were removed. This mask was then applied to the 120 kHz echogram resulting in the isolation of aggregations. For comparisons between schools, all energetic (i.e., NASC, TS) and positional (i.e., longitude, latitude, distance from bottom, vertical position in water column or depth) descriptors were exported from the post-filter 120 kHz echogram.

The Echoview Single-target detection method 2 algorithm was used for single target analysis. Parameters used to filter out single targets were relaxed from recommended settings (Ona and Barange, 1999) due to the observed patchiness of schools and number of single targets per bin. Single targets outside a maximum beam compensation of 3 dB, normalized pulse length between 0.60 and 1.50, phase

deviation of 1 step, and a minimum TS threshold of -60 dB were rejected. An additional algorithm was adapted using the Sawada Index (N_V) which represents the number fish per reverberation volume (Sawada *et al.* 1993). All single target TS values in cells with $N_V > 0.10$ were rejected.

Abundance and Biomass Estimation

A multi-step approach was used to estimate menhaden abundance and biomass based on acoustic measurements. Mean NASC for each sampling month was calculated using a method for stratified analysis of multiple strata adapted from Jolly and Hampton (1990). Each survey was split up into approximately longitudinal (i.e., eastward and westward) transect segments ($N = 228$ across all surveys). NASC from menhaden schools along each transect were weighted based on their school-to-transect length ratio and then averaged. The first and second strata consisted of calculated the daily and monthly mean NASC at each site respectively. Daily mean NASC was estimated by taking a weighted-mean via

$$\widehat{\overline{NASC_{ik}}} = \frac{1}{n_i}\sum_{j=1}^{n_{ik}} w_{ijk}\,\widehat{\overline{NASC_{ijk}}} \quad (1),$$
$$w_{ijk} = \frac{L_{ijk}}{\frac{1}{n_{ik}}\sum_{j=1}^{n_{ik}} L_{ijk}},$$

where $\widehat{\overline{NASC_{ik}}}$ is the mean NASC for the *i*th day at site *k*, n_i is total number of transects within the stratum, w_{ijk} is the weight applied to the *j*th transect, *L* is the along-track distance (m) of each transect line. The monthly mean was estimated using a slightly modified form of equation (1) where $\widehat{\overline{NASC_{ijk}}}$ is now represents the *j*th daily mean NASC during at site *k* the *i*th month. The third and final stratum consisted of estimating the mean between both sites:

$$\widehat{\overline{NASC_i}} = \frac{\sum_k S_{ik}\widehat{\overline{NASC_{ik}}}}{\sum_k S_{ik}} \quad (2),$$

where S_{ik} is the total survey length at site *k* during the *i*th month.

Monthly mean σ_{bs} (the acoustic scattering cross-section [m^{-2}] and the linear transform of TS), was calculated by weighting daily site σ_{bs} means by their respective survey length. The areal fish numerical density (ρ_A, fish/m^2) was then estimated via:

$$\rho_A = \frac{\widehat{\overline{NASC_i}}}{4\pi\sigma_{bs}(1852)^2} \quad (3),$$

where $\widehat{\overline{NASC_i}}$ represents both the combined and individual monthly mean NASC for the sampling sites. Numeric menhaden abundance was calculated via $N = \rho_A A$ (Simmonds and MacLennan 2006) where N is the monthly abundance (# fish) and A is the total site area (km^2). In order to calculate biomass, monthly mean σ_{bs} was transformed to TS and converted into a comparable standard fish length (cm) using a TS-length model. However, due to the absence of a dorsal TS-length model specific to Atlantic menhaden, several published models for clupeoids were considered and compared (Table 2). The monthly mean fish length was then used to estimate monthly mean fish wet-weight using an empirical weight-length relationship specific to Atlantic menhaden (ASMFC 2010):

$$\ln(W) = -11.029\mathrm{TL}_{\mathrm{TS}}^{3.010}(4),$$

where W is mean weight in grams and TL_{TS} is the mean TS-derived fish length (mm). Biomass (kg) was then estimated by first converting W into kilograms and then multiplying by abundance: $B = NW_{kg}$.

Table 2. TS-length models at 120 kHz used in other studies for clupeoids where L is length (cm).

Fish Species	Equation	Literature Source
Generalized formula	$19.1\log_{10}(L) + 0.9\log_{10}(\lambda) - 63.88$[a]	Love (1971)
Mixed clupeoid and non-clupeoid		
Alewife, smelt, bloater	$19.1\log_{10}(L) - 64.9$	Brandt *et al.* (1991)
Clupeoid		
Herring	$18.8\log_{10}(L) - 62.4$	Nakken and Olsen (1977)
Herring	$26.2\log_{10}(L) - 72.5$	Thomas *et al.* (2002) [1]
Herring	$20\log_{10}(L) - 66.0$	Thomas *et al.* (2002) [2]
Herring, sprat	$20\log_{10}(L) - 76.0$	Appenzeller and Leggett (1992)
Herring, sprat	$20\log_{10}(L) - 73.1$	Degnbol *et al.* (1985)[1]
Herring, sprat	$20\log_{10}(L) - 73.4$	Lassen and Stæhr (1985)[1]

[a] λ is the acoustic wavelength in cm
[1] *In-situ* observations

The monthly coefficient of variation (*CV*) for NASC was calculated using

$$CV = \frac{\sqrt{Var(\widehat{NASC_i})}}{\widehat{NASC_i}}(5),$$

where *i* represents the stratum and $Var(\widehat{NASC_i})$ is the variance in NASC where:

$$Var(\widehat{NASC_i}) = \frac{\sum_i S_{ik}^2 (\sum_{k=1}^{n_{ik}} w_{ik}^2 \frac{(\widehat{NASC_{ik}} - \widehat{NASC_{ik}})^2}{n_{ik}(n_{ik}-1)})}{(\sum_i S_{ik})^2}.$$

Total uncertainty, or the combined standard uncertainty (CSU), for extrapolated monthly abundance and biomass estimates was calculated using the 'root sum squared' (RSS) method (Taylor and Kuyatt 1994):

$$u(N_i \vee B_i) = \sqrt{[u\frac{(\widehat{NASC_i})}{\widehat{NASC_i}}]^2 + [u\frac{(\sigma_{bs_i})}{\overline{\sigma_{bs_i}}}]^2 + [u\frac{(L_i)}{\overline{L_i}}]^2}\ (6),$$

where terms in the numerator and denominator represent the standard uncertainty and mean for the *i*th month respectively. A Type A evaluation of uncertainty (Taylor and Kuyatt 1994) was used to estimate standard uncertainties for each term:

$$u(\widehat{NASC_i}) = \frac{[\sqrt{Var(\widehat{NASC_i})}]}{[\sqrt{n_i}]}(7),$$

$$u(\sigma_{bs_i} \vee L_i) = \frac{\sigma_i}{[\sqrt{n_i}]} \text{ (8)},$$

where i is the month, σ_i is the standard deviation, and n_i is the number of samples for each term.

Statistical Analysis

Descriptive statistics (i.e., mean, medians, measures of dispersion) were used on a school-by-school basis to examine school NASC (m^2 nmi^{-2}), length (m), thickness (m), and mean depth (m). A Spearman (ρ, $\alpha = 0.05$) correlation coefficient test was used to describe any significant relationships between school parameters. The spatial structure of menhaden schools was characterized using a cluster coefficient which was estimated by

$$C_{dr} = \frac{\overline{NND}}{\overline{MND}} \text{ (9)},$$

where C_{dr} is the daily cluster coefficient, NND is the mean nearest neighbor distance, and MND is the mean between all schools. Values of C_{dr} range from 0 to 1 and represent extremely clustered and dispersed schools respectively. The C_{dr} was calculated daily for each region where more than 1 school was encountered. Descriptive statistics of how menhaden were distributed by transects (normalized to schools per km of transect). Significant differences in the monthly mean NASC and TS (in the linear domain) between survey months and sites was tested using a type II analysis of variance (ANOVA, $\alpha = 0.05$). A *post hoc* Tukey's Honest Significance Test (Tukey HSD, $\alpha = 0.05$) was used for pairwise comparisons between survey months and sites.

Results

School Characteristics

School NASC was the most variable parameter (mean = 35,700 m^2 nmi^{-2}, $CV = 1.63$) which ranged between 600 and 396,000 m^2 nmi^{-2} (Table 3). Between schools of similar dimensions two qualitative "school-types" were observed based on their respective NASC: dense ($n = 22$) and diffuse ($n = 63$) (Figure 3). Schools with NASC values exceeding the 75th percentile of all NASC values (~40,000 m^2nmi^{-2}) were considered to be "dense" whereas the remainder were identified as "diffuse". Mean school thickness of dense schools (3.3 m, $CV = 0.10$) was significantly greater than their diffuse counterparts (2.3 m, $CV = 0.05$; t-test, $t = 3.00$, $p < 0.01$). Otherwise, there were no significant differences in school length ($t = 1.42$, $p = 0.16$) or depth ($t = -1.77$, $p = 0.08$). There was moderate variability in both school length (mean = 17.5 m, $CV = 0.75$) and thickness (mean = 2.6 m, $CV = 0.46$) that ranged from 2.5 to 68.8 and 0.9 to 5.9 m respectively. There was a moderate correlation between school NASC and thickness ($\rho(85) = 0.50$, $p < 0.01$). Conversely, the relationship between NASC and length was relatively weak ($\rho(85) = 0.32$, $p < 0.01$). Another feature of these schools was the spectrum of aspect ratios (length/thickness) that resulted from the relative variability in these two school dimensions. Aspect ratios ranged from 0.96 (roughly symmetrical) to 20.70 (horizontally long, vertically compressed) resulting in a distribution of generalized shape parameters that was independent of depth ($\rho(85) = -0.14$, $p = 0.22$). There was no significant correlation between school aspect ratio and NASC ($p(85) = 0.02$, $p = 0.82$). Variability in the mean depth (mean = 5.9 m, $CV = 0.46$) was similar to thickness with schools ranging from 2.9 to 17.9 m in depth. There were no significant correlations

between depth and school length ($\rho(85) = 0.15$, $p = 0.17$) and NASC ($\rho(85) = -0.16$, $p = 0.13$); however, there was a significant relationship between school thickness and depth ($\rho(85) = 0.46$, $p < 0.01$).

Table 3. Descriptive statistics for school NASC, length, thickness, and mean depth. Asterisks indicate significant differences (*t*-test, $p < 0.05$) in the respective parameter between diffuse and dense schools.

School Parameters								
Statistic	**NASC (m^2 nmi^{-2})***		**Length (m)**		**Thickness (m)***		**Depth (m)**	
	Diffuse	Dense	Diffuse	Dense	Diffuse	Dense	Diffuse	Dense
Mean	14,500	96,500	21.6	15.9	2.3	3.3	6.1	5.2
CV	0.09	0.20	0.06	0.07	0.05	0.09	5.5	4.9
Median	12,200	63,400	12.0	13.9	2.3	3.3	0.06	0.07

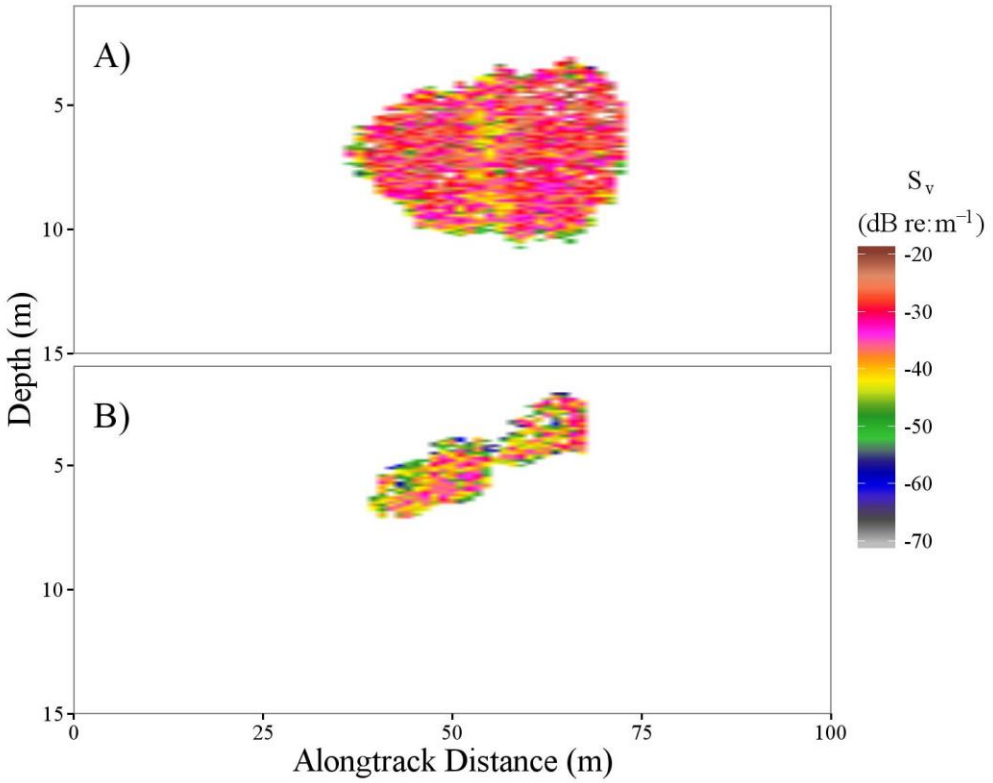

Figure 3. Maximum school NASC observed was 397,000 m^2 nmi^{-2} on 16 August 2014 at Atlantic Beach from a 35.5 x 7.5 m (length x height) aggregation (**A**) which was an order of magnitude greater than a similarly-sized school (31.5 x 5.5 m) (**B**) comprising a NASC of 20,000 m^2 nmi^{-2},

Overall, there was relatively high variability in both mean NND (250 m, $CV = 1.0$) and C_{dr} (0.26, $CV = 0.62$) among surveys and regions (Figure 4). Qualitatively, there were three patterns of clustering of observed schools among surveys: high ($C_{dr} \leq 0.1$), moderate ($0.1 < C_{dr} \leq 0.3$), and low ($C_{dr} > 0.3$) clustering. Likewise, significant differences in mean NND were detected among survey months ($F_{(6,72)} = 7.2$, $p < 0.01$) but not between regions ($F_{(1,72)} = 1.5$, $p = 0.23$). The lack of significant difference between regions and no clear seasonal trend (i.e., April to September) represents the patchiness and

high variability in schools both in space and time. The relative range between maximum (NND = 50 m, C_{dr} = 0.06) and minimum (NND = 550 m, C_{dr} = 0.49) NND and C_{dr} suggests that schools were always clustered to some degree.

These patterns in clustering were also reflected in how schools were distributed among transects. A total of 70 transects (out of 228 transects included in this analysis) had schools with 48 having at least one school and the remaining 22 consisting of two or more. A maximum of six schools for one transect was observed on 12 August 2015 at Atlantic Beach compared to the overall mean of 1.8 schools per transect (CV = 0.61). When normalized to the length of each transect, there was relatively high variability to number of schools per transect-km (mean = 1.1 schools/transect-km, CV = 1.20). Similar to the absolute number of schools per transect, the maximum schools per transect-km was observed on 12 August 2015 at Atlantic Beach (mean = 9.0 schools/transect-km). Likewise, there was a strong correlation between survey C_{dr} (and therefore NND) and the mean normalized transect school density ($\rho(9) = -0.78$, $p = 0.01$; Spearman). However, there was no significant correlation between mean transect NASC and C_{dr} ($\rho(9) = -0.45$, $p = 0.22$) or transect school density ($\rho(9) = 0.62$, $p = 0.08$; Figure 5). Lastly, disparity between CV estimates for nearest and mean neighbor distances (0.63 and 0.24 respectively) resemble differences between absolute and normalized transect school densities (1.20 and 0.61 respectively).

Significant differences in mean transect NASC were significantly different among survey months ($F_{6,144} = 3.0$, $p = 0.01$, ANOVA), regions by survey months ($F_{6,144} = 3.9$, $p < 0.01$). but not between regions ($F_{6,144} = 0.1$, $p = 0.83$). Mean transect NASC during August (2,500 m^2 nmi^{-2}, CV = 0.36) and September 2015 (4,800 m^2 nmi^{-2}, CV = 0.71) were significantly greater than during April, May, and June 2015 ($p < 0.05$; Tukey HSD). Likewise, at Atlantic Beach mean transect NASC during August 2015 (8,500 m^2 nmi^{-2}, CV = 0.28) was significantly greater than during August 2014 (400 m^2 nmi^{-2}, CV = 0.72; $p < 0.01$), April, May, and June 2015 (~0 m^2 nmi^{-2}; $p < 0.01$; Figure 6).

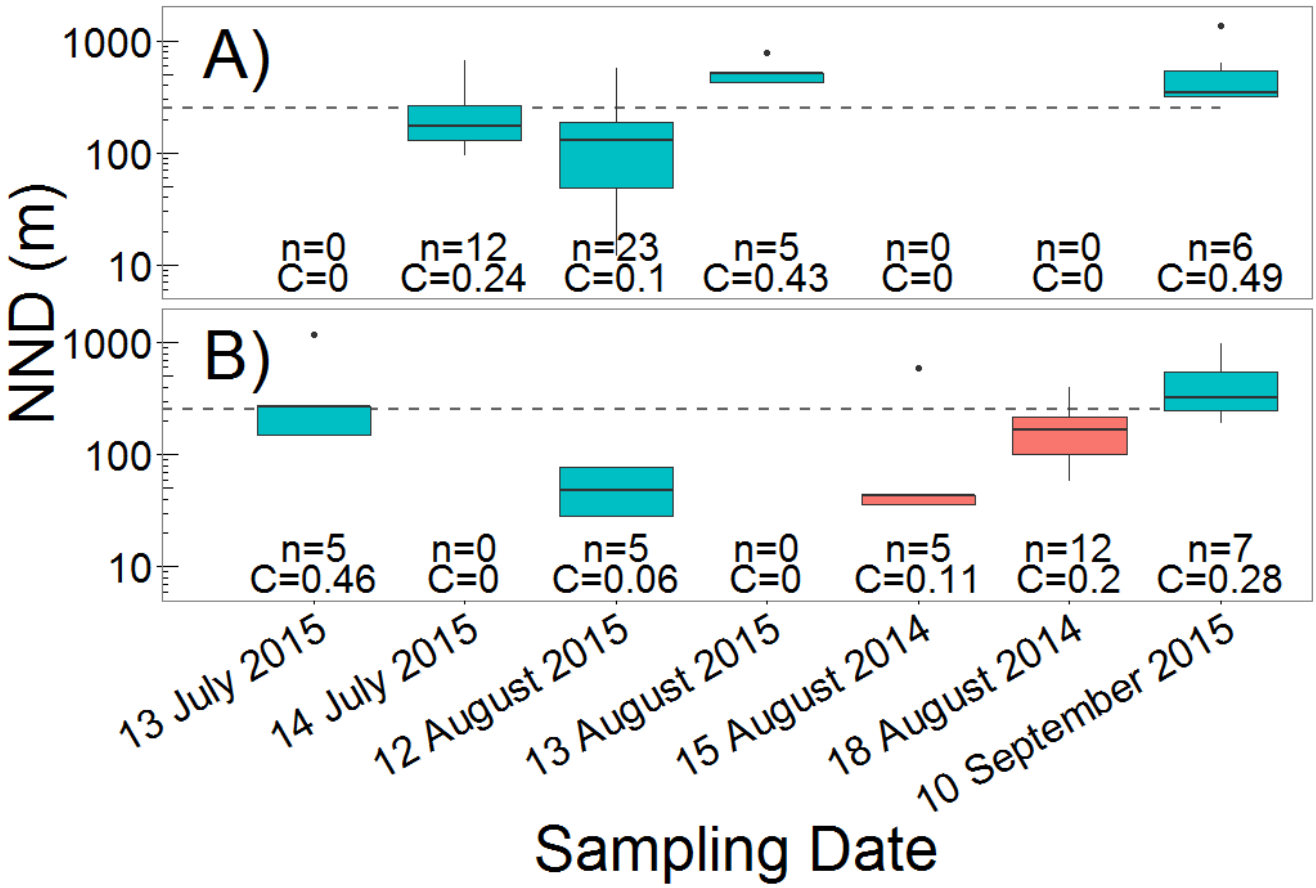

Figure 4. There was evidence of spatial clustering via nearest neighbor distances (NND) between menhaden schools that varied among sampling months at (**A**) Atlantic Beach and (**B**) Hempstead. The horizontal black line for each box represents the median while the limits of the box represents the interquartile range (25-75%). The dashed horizontal line represents the median TS for all surveys. Red and blue regions represent data from 2014 and 2015 respectively. C represents the C_{dr} coefficient.

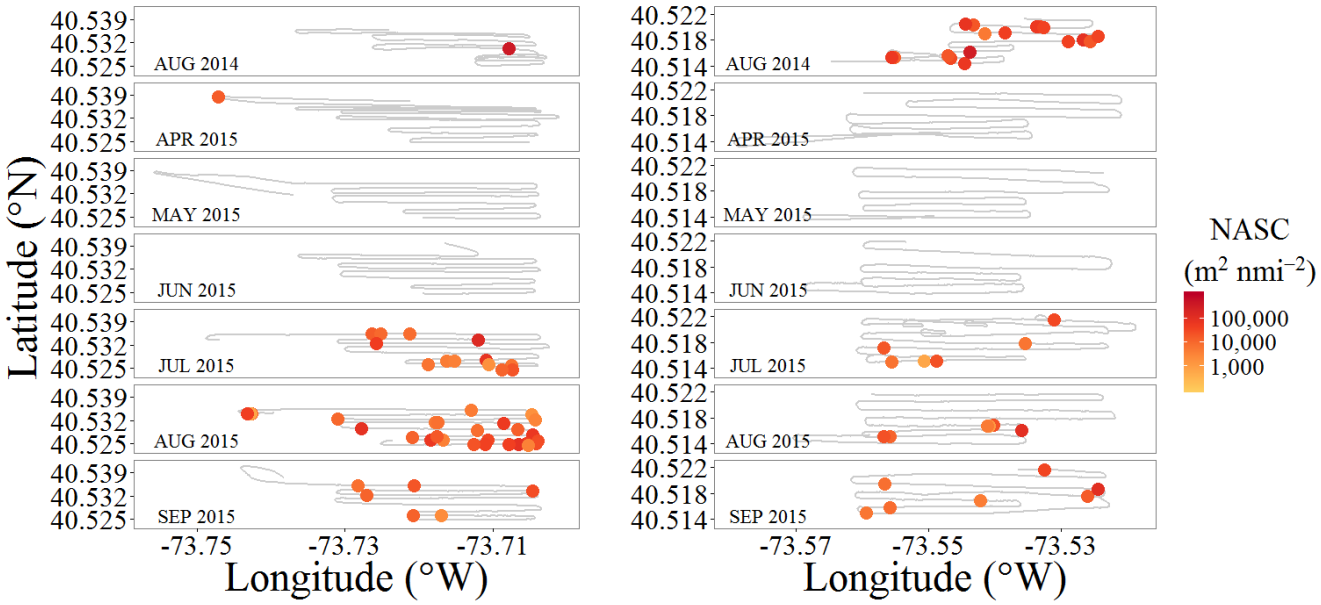

Figure 5. Spatial distribution of schools during each sampling month. Each column represents (**left**) Atlantic Beach and (**right**) Hempstead. Color of each point is scaled to the integrated NASC for each school. Gray lines represent a sample cruise track from each month and site.

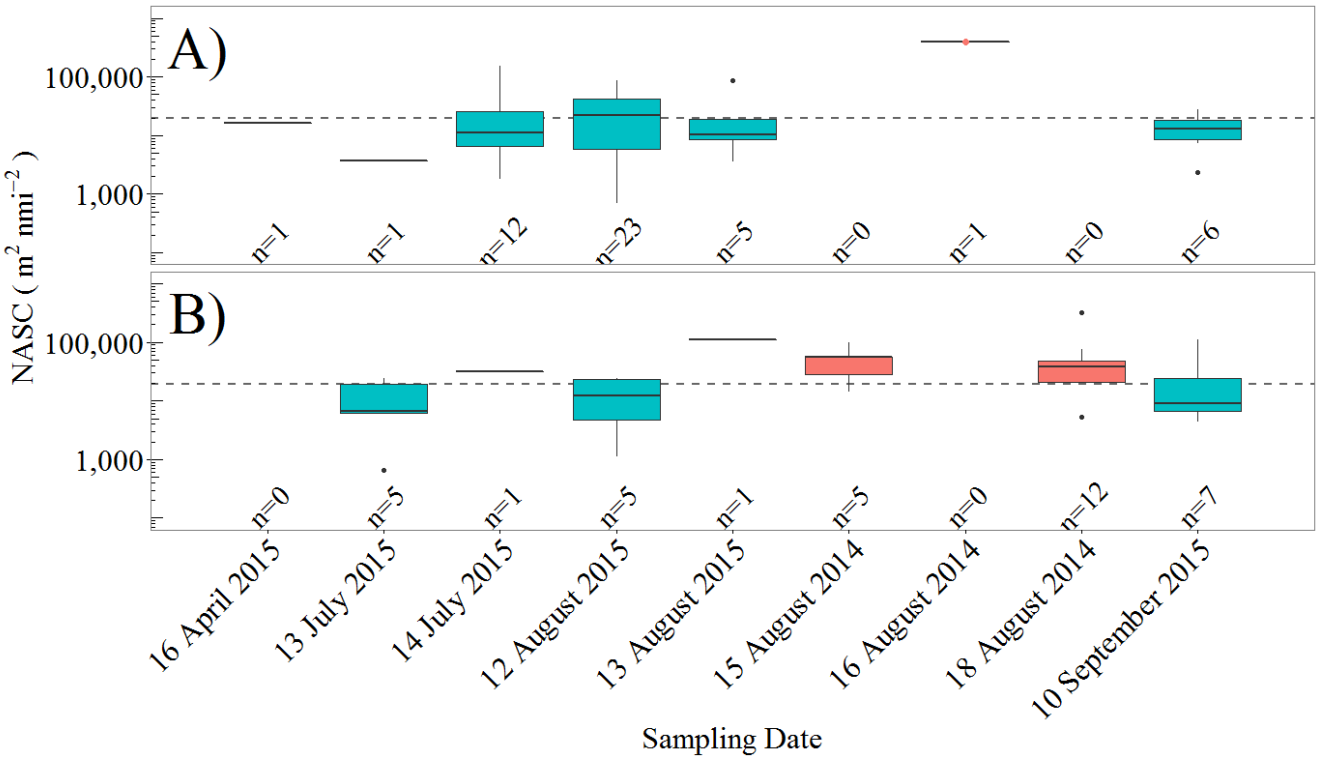

Figure 6. Weighted mean NASC varied significantly among survey months at (**A.**) Atlantic Beach and (**B.**) Hempstead. The horizontal black line for each box represents the median while the limits of the box represents the interquartile range (25-75%) of non-zero NASC transects. The dashed horizontal line represents the median transect NASC for all surveys. Red and blue regions represent data from 2014 and 2015 respectively. Values of *n* represent the number of non-zero NASC transects. No schools were detected in May or June 2015.

In-situ Target Strength

Significant differences in mean single target TS were detected among survey months ($F_{1,2774} = 72.2$, $p < 0.01$; ANOVA), sites ($F_{1,2774} = 19.2$, $p < 0.01$), and the interaction between the two $F_{1,2774} = 133.9$, $p < 0.01$). Mean TS during August 2014 at Atlantic Beach (-32.75 dB, $N = 68$) was significantly higher than all observed *in situ* TS during any other month at either site (Tukey HSD, $p < 0.01$). At Atlantic Beach mean TS during August 2015 (-40.64 dB, $N = 1{,}491$) was significantly higher than both July (-43.51 dB, $N = 218$; $p < 0.01$) and September 2015 (-41.88, $N = 168$; $p = 0.03$). There were no significant differences in mean TS between months at Hempstead ($p > 0.05$; Figure 4). Between sites, mean TS at Hempstead during July (-35.69 dB, $N = 57$) and August 2015 (-44.87 dB, $N = 241$) were significantly greater and smaller than at Atlantic Beach during August 2015 ($p < 0.01$) respectively. Consequently, these significant results validated the use of mean TS for each separate sampling region and month for subsequent calculations of abundance and biomass.

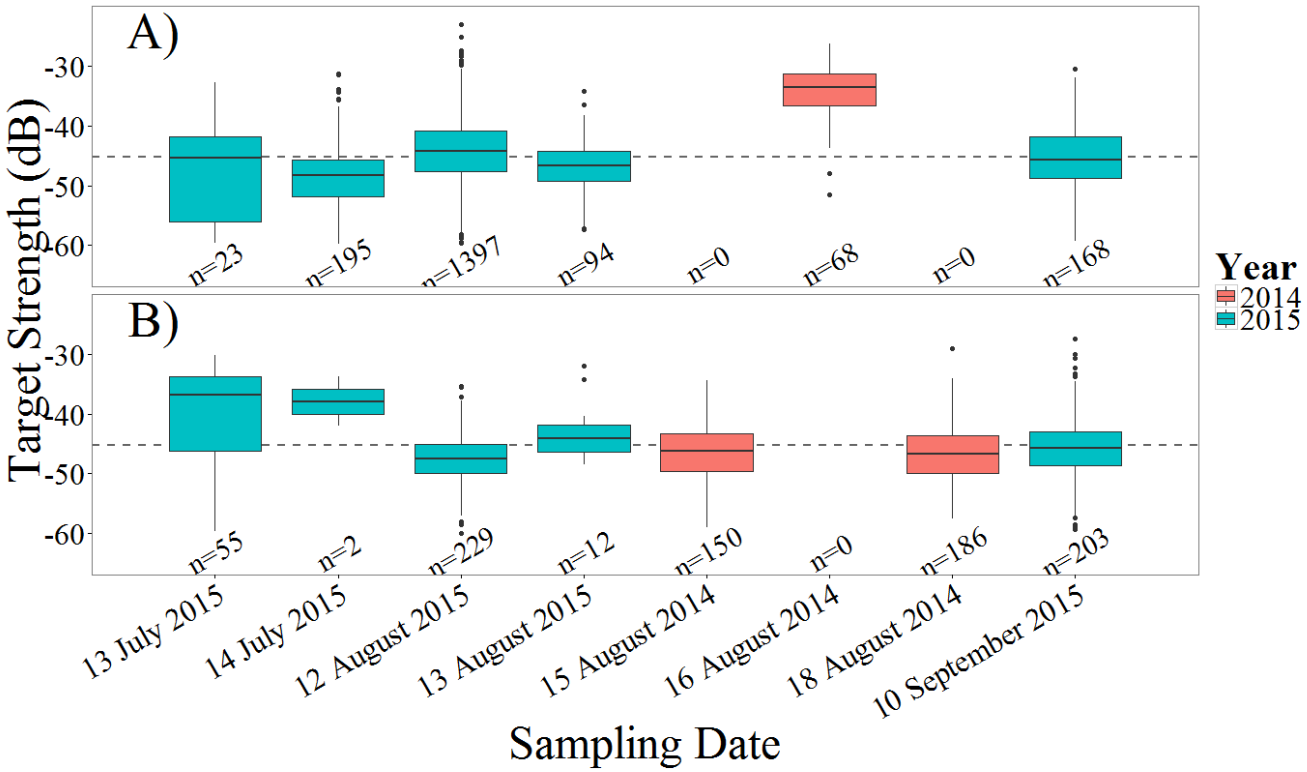

Figure 7. *In situ* TS varied significantly among sampling months at (**A.**) Atlantic Beach and (**B.**) Hempstead. The horizontal black line for each box represents the median while the limits of the box represents the interquartile range (25-75%). The dashed horizontal line represents the median TS for all surveys. Red and blue regions represent data from 2014 and 2015 respectively. No single target TS values were detected during April, May, or June 2015.

Abundance and Biomass Distributions

The choice of TS-length model had a considerable effect on biomass estimates. Variability across biomass estimates from different models was consistently high ($CV \sim 1.41$). Models from Degnbol *et al.* (1985) and Lassen and Stæhr (1985) were relatively consistent with one another ($CV \sim 0.07$) but produced biomass estimates approximately two orders of magnitude greater than any of the other models. The Love (1971), Brandt *et al.* (1991), and Thomas *et al.* (2002) models were also similarly consistent with one another ($CV \sim 0.04$). Compared to these three models, models from Nakken and Olsen (1978) and Thomas *et al.* (2002) under- ($CV \sim 0.27$) and over-estimated ($CV \sim 0.26$) biomass estimates respectively. Consequently, the mean output from Love (1971), Brandt *et al.* (1991), and Thomas *et al.* (2002) was used to extrapolate biomass.

Extrapolated biomass for the Atlantic Beach and Hemsptead survey areas varied with no apparent trend in time aside from their general absence between April and July (Table 4). During August 2014 peak biomass and abundance was observed at Hempstead which were both two orders of magnitude greater than what was observed at Atlantic Beach. During 2015 the combined biomass and abundance increased over the course of the summer. Between the two sites biomass and abundances were highest at Atlantic Beach during July and August and at Hemsptead during September 2015. Overall, when taking into account maximum uncertainty monthly (22.8-49.7%) summer estimates in 2014 and 2015 ranged from 7,190,000 to 12,030,000 and from 1,120,000 to 10,780,000 fish respectively at each study

site. Likewise, summer estimates of biomass in 2014 and 2015 at each site ranged from 953,000 to 1,595,000 and from 92,500 to 596,600 kg respectively.

Table 4. Extrapolated abundance (# fish), biomass (kg), and uncertainty (%) for Atlantic Beach and Hempstead during each sampling month. Combined represents the weighted mean output from both Atlantic Beach and Hempstead using equation (2).

	Atlantic Beach			**Hempstead**		
Survey Month	*N* (# fish)	*B* (kg)	*CSU* (%)	*N* (# fish)	*B* (kg)	*CSU* (%)
Aug-14	120,000	16,400	*21.0*	11,050,000	1,465,000	*15.2*
Apr-15	1,000	100	*33.4*	0	0	*0.0*
May-2015	0	0	*0.0*	0	0	*0.0*
Jun-2015	0	0	*0.0*	0	0	*0.0*
Jul-2015	1,270,000	102,700	*21.9*	260,000	21,000	*24.9*
Aug-2015	4,160,000	266,400	*12.3*	800,000	51,300	*19.2*
Sep-2015	920,000	51,100	*28.4*	4,820,000	267,100	*40.7*

Discussion

There was evidence of relatively high spatial variability and clustering between schools that varied over time. Similar to the relative patchiness of other schooling fish species such as Walleye pollock (Shen *et al*. 2008), menhaden schools were ephemeral with a maximum along-track distance of approximately 70 meters. Likewise, NASC estimates of schools were consistent with the relative numeric fish densities associated with menhaden (Figure 8). Clustering was relatively moderate to high ($C_{dr} \leq 0.3$) for a majority of menhaden schools and was independent of clustered fish school characters such as length, thickness, mean depth, and integrated NASC. This result differs from observed clustering in other fish species (Shen *et al.* 2008); however, it is unclear how observed clustering in this study reflect standard spatial heterogeneity of menhaden schools due to the relatively high degree of variability. Likewise, clustering did not appear to coincide with changes in school presence over the course of the summer from July to September.

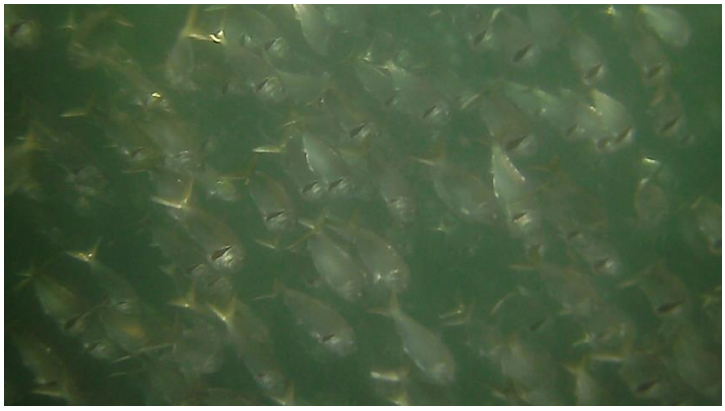

Figure 8. Menhaden school observed in the coastal waters of Long Island during September 2015. Frame captured from video courtesy of Dr. Mark Bond.

The presence of menhaden schools at Hempstead and Atlantic Beach were mostly concentrated during August and September 2015; peak school counts for both sites occurred during August (2014 and 2015 for Hempstead and Atlantic Beach respectively). Even though the explicit spatial and temporal distribution of menhaden in New York coastal waters isn't well represented in the literature, our observations of schools confirmed the presence of menhaden during the summer months with an outlier in April 2015. Moreover, increasing presence of menhaden from spring into fall is consistent with numerous observations and studies across numerous estuaries along their geographic range (Ahrenholz 1991; McHugh 1972). Aside from outliers the mean *in situ* TS, a proxy measurement for general size class of these schools, did not vary significantly between sampling months and regions.
This is consistent with ecological observations of offshore menhaden whereby schools in coastal waters mostly comprise adults whereas age-0 and younger fish are in the estuaries during summer months (Ahrenholz 1991). Since the growth rate of adult menhaden is significantly slower than that of age-0 fish, it would be expected that the overall TS distribution would not undergo large shifts due to a relatively consistent age class of similar size ranges. Likewise, non-significant differences in mean TS between survey regions suggests that there was no spatial age class separation either.

There were, however, two exceptions. First, single target TS measurements from Atlantic Beach on August 2014 were significantly greater than all other sub-samples except for Hempstead on July 2015. Second, mean TS from Hempstead on July 2015 was significantly greater than Atlantic Beach during the same month. The August 2014 TS measurements comprised a single school, dense school which had a mean TS of -32.8 dB and NASC of approximately 400,000 m^2 nmi^{-2}. Although other factors such as three-dimensional orientation and swim bladder morphology/physiology could also be having an impact on mean TS, it is probable that not all biased single target TS values were removed from this school and resulted in a relatively skewed distribution. For the second exception, one out of the six schools observed had mostly single target TS values exceeding -38.0 dB while the remaining schools were primarily less than -42.0 dB. Similar to the first exception, it is probable that some of these TS values remained biased due to multiple scattering in conjunction with other aforementioned sources of error.

Non-significant differences in mean transect NASC between sampling sites suggest that the influx of menhaden biomass into our survey regions during the mid-summer is constant and that transect school densities were similar. This is further exemplified with there being no significant change in NASC between July and September 2015. Conversely, while there was no significant change in overall mean

NASC between August 2014 and 2015, peak NASC at Atlantic Beach during August 2015 was significantly higher than any other month. This also coincided with a peak number of schools and clustering as well which may have contributed this relatively high density. In terms of biomass and abundance, the same general trends apply with the exception of August 2014 comprising the highest values.

Due to their northward coastal migration, it was possible to encounter menhaden in mid- to late-spring; however, with the exception of one school in April, no schools were observed in May and June. That may have been a result of the range of distances from shore menhaden spawn which can vary from relatively near- (< 8 km) to far off-shore (~50 km) in both the spring and autumn months (Quinlan *et al.* 1999). Likewise, observations of this migration suggest that menhaden move through the Mid-Atlantic Bight as quickly as 1 to 2 months which could account for their sudden presence in large numbers. Conversely, under-sampling of schools may have been a consequence of the generally patchy distribution of schools. These potential sources of error were not depicted in our estimated of combined uncertainty.

Assuming that the total biomass/km^2 for each sampling date during 2015 is representative of the overall coastal distribution of menhaden along Long Island (~15 km offshore, ~194 km along-coast) a regional (NY coastal waters) total biomass could be estimated. This menhaden biomass ranged from 60,000 kg in April to 345,980,000 kg in September. The predicted offshore southward migration of menhaden in the late summer and early fall (Ahrenholz 1991) supports peak estimates of menhaden during September. Comparatively, our estimate of biomass along coastal Long Island represented up to approximately 24% of the total stock biomass estimate (~ 1.5 billion kg) according to the 2015 stock assessment report (SEDAR 2015). However, this rough estimation hinges on the assumption of uniform areal biomass density along the entirety of coastal Long Island which is unlikely.

Improving methods for estimating menhaden abundance and biomass from fine to broad spatiotemporal resolutions is critical for successful EBFM implementation. For instance, multispecies and ecosystem-level models used in the northwest Atlantic (e.g., MSVPA-X, NEFSC 2006) include menhaden distributions as being a key ecological component for the stocks of higher trophic species such as bluefin tuna (Butler *et al.* 2010), striped bass (Sanchirico *et al.* 2007), weakfish, and bluefish (NEFSC 2006). The availability of menhaden to predators, along with other forage fish species, also has substantial impacts on populations of seabirds, marine mammals, and ultimately humans (Alder *et al.* 2008). Collapses of the menhaden population in the 1950's (McHugh 1972; SEDAR 2015) along with the general depletion of other forage fish (Essington *et al.* 2015) raise concerns for these higher trophic species. Although there are additional uncertainties not factored into our biomass estimates such as the broader, coastal spatial structure of migrating menhaden, acoustic estimates of biomass could be useful in quantifying near-shore ecosystem dynamics along the southern coast of Long Island, namely food availability for higher trophic level organisms such as marine mammals and other piscivores.

Conclusion

This study provides acoustic estimates of in situ TS, biomass, and fish numerical density for Atlantic menhaden in coastal waters. Once menhaden schools were present during the summer months they remained in high numbers and biomass with a peak in August 2015. Due to the patchiness of menhaden schools, surveys with greater sampling coverage are needed to provide more accurate spatial and temporal information on menhaden biomass and abundance in coastal waters south of Long Island.

Acoustic estimates of abundance and biomass can provide quantitative data useful for better understanding how estuarine and oceanic trophic webs are linked through forage fish such as menhaden and enhanced ecosystem-based approaches to fisheries management.

References

Alder J., Campbell B., Karpouzi V., Kaschner K., and Pauly D. (2008). *Forage fish: From ecosystems to markets*. Annual Review of Environment and Resources, 33: 153-166.

Ahrenholz D., Nelson W., and Epperly S. (1987). *Population and fishery characteristics of Atlantic menhaden, Brevoortia tyrannus*. Fishery Bulletin, 85(3), 569-600.

Ahrenholz D. (1991). *Population biology and life history of the North American menhadens, Brevoortia spp.* Marine Fisheries Review, 53(4), 3-19.

Appenzeller A. and Leggett W. (1992). *Bias in hydroacoustic estimates of fish abundance due to acoustic shadowing: evidence from day-night surveys of vertically migrating fish*. Canadian Journal of Fisheries and Aquatic Sciences, 49, 2179-2189.

Atlantic States Marine Fisheries Commission (ASMFC). (2010). *Atlantic menhaden stock assessment for peer review*. Stock Assessment Report No. 10-02.

Atlantic States Marine Fisheries Commission (ASMFC). (2012). *2012 Atlantic stock assessment update*. Atlantic State Marine Fisheries Commission, Washington, D.C.

Baxter J. and Batty R. (1990). *Swimbladder "behaviour" and target strength*. Rapports et procès-verbaux des réunions / Conseil permanent international pour l'exploration de la mer, 189: 233-244.

Bezerra-Neto J., Brighenti L., and Pinto-Coelho R. (2013). *Implementation of hydroacoustic for a rapid assessment of fish spatial distribution at a Brazilian lake – Lagoa Santa, MG.* Acts Limnologica Brasilienia, 25: 91-90.

Brandt S., Mason D., Patrick E., Argyle R., Wells L., Unger P., and Stewart D. (1991). *Acoustic measures of the abundance and size of planktivores in Lake Michigan.* Canadian Journal of Fisheries and Aquatic Sciences, 48, 894-908.

Bortman M. and Niedowski N. (1998). *Characterization Report of the Living Resources of the Peconic Estuary.* Peconic Estuary Program, Suffolk County Department of Health Services, Riverhead, NY.

Boswell K., Wilson M., and Wilson C. (2007). *Hydroacoustics as a tool for assessing fish biomass and size distribution associated with discrete shallow water estuarine habitats in Louisiana*. Estuaries and Coasts, 40: 1-11.

Bucheister A., Miller T., Houde E., Secor D., and Latour R. (2016). *Spatial and temporal dynamics of Atlantic menhaden (Brevoortia tyrannus) recruitment in the Northwest Atlantic Ocean*. ICES Journal of Marine Science, 73: 1147-1159.

Butler C., Rudershausen P., and Buckel J. (2010). *Feeding ecology of Atlantic blue fine tuna (Thunnus thynnus) in North Carolina: diet, daily ratio, and consumption of Atlantic menhaden (Brevoortia tyrannus)*. Fishery Bulletin, 108: 56-69.

Coasta B., Taylor J., Kracker L., Battista T., and Pittman S. (2014). *Mapping reef fish and the seascape: Using acoustics and spatial modeling to guide coastal management*. PLoS One, 9: e85555.

Cressie N. (1993). *Statistic for spatial data.* Wiley, New York. 900 pp.

Degnbol P., Lassen H., and Stæhr K. (1985). *In situ determination of target strength of herring and sprat at 38 and 120 kHz*. Dana, 5: 45-54.

Demer D., Zwolinski J., Cutter G. Jr., Byers K., Macewicz B., and Hill K. (2013). *Sampling selectivity in acoustic-trawl surveys of Pacific sardine (Sardinops sagax) biomass length distribution*. ICES Journal of Marine Science, 70: 1369-1377.

Duncan A. and Kubecka J. (1996). *Patchiness of longitudinal fish distributions in a river as revealed by a continuous hydroacoustic survey*. ICES Journal of Marine Science, 53: 161-165.

Essington T., Moriarty P., Froehlich H., Hodgson E., Koehn L., Oken K., Siple M., and Stawitz C. (2015). *Fishing amplifies forage fish population collapses*. Proceedings of the National Academy of Sciences of the United States of America, 112: 6648-6652.

Fernandes P. (2009). *Classification trees for species identification of fish-school echotraces*. ICES Journal of Marine Science, 66: 1073-1080.

Ferraro S. (1979). *Daily time of spawning of 12 fishes in the Peconic bays, New York*. Fishery Bulletin, 78: 455-464.

Foote K., Knutsen H., Vestnes G., MacLennan D., and Simmonds E. (1987). *Calibration of acoustic instruments for fish density estimation: a practical guide.* Cooperative Research Report, ICES 144.

Foote K., Ona E., and Toresen R. (1992). *Determining the extinction cross section of aggregating fish*. The Journal of the Acoustical Society of America, 81: 1983-1989.

Friedland K., Lynch P., and Gobler C. (2011). *Time series mesoscale response of Atlantic menhaden Brevoortia tyrannus to variation in plankton abundances*. Journal of Coastal Research, 27: 1148-1158.

Gabriel R. (1921). *The evolution of Long Island: A story of land and sea*. New Haven, CT: Yale University Press.

Goode G. (1880). *A history of the menhaden*. Orange Judd Company, New York, NY.

Guillard J. and Lebourges A. (1998). *Preliminary results of fish population distribution in a Senegalese coastal area with depths less than 15 m, using acoustic methods*. Aquatic Living Resources, 11: 13-20.

Guillard J.,m Simier M., Albaret J., Raffray J., Sow I., and Morais T. (2012). *Fish biomass estimates along estuaries: A comparison of vertical acoustic sampling at fixed stations and purse seinse catches.* Estuarine, Coastal and Shelf Science, 107: 105-111.

Handegard N., Buisson L., Brehmer P., Chalmers S., De Robertis A., Huse G., Kloser R., Macaulay G., Maury O., Ressler P., Stenseth N., and Godo O. (2012). *Towards an acoustic-based coupled observation and modelling system for monitoring and predicting ecosystem dynamics of the open ocean*. Fish and Fisheries, 14: 605-615.

Hartman K. and Brandt S. (1995). *Trophic resource partitioning, diets, and growth of sympatric estuarine predators*. Transactions of the American Fisheries Society, 124: 520-537.

Jackson J., Kirby M., Berger W., Bjorndal K., Botsford L., Bourque B., Bradbury R., Cooke R., Erlandson J., Estes J., Hughes T., Kidwell S., Lange C., Lenihan H., Pandolfi J., Ptereson C., Steneck R., Tegner M., and Warner R. (2001). *Historical overfishing and the recent collapse of coastal ecosystems*. Science, 293: 629-637.

Jech J., Price V., Chavez-Rosales S., and Michaels W. (2015). *Atlantic herring (Clupea harengus) demographics in the Gulf of Maine from 1998 to 2012*. Journal of Northwest Atlantic Fishery Science, 47: 37-54.

Jolly G. and Hampton I. (1990). *A stratified random transect design for acoustic surveys of fish stocks*. Canadian Journal of Fisheries and Aquatic Sciences, 47: 1282-1291.

Krumme U. and Saint-Paul U. (2003). *Observations of fish migration in a macrotidal mangrove channel in Northern Brazil using a 200-kHz split-beam sonar*. Aquatic Living Resources, 16: 175-184.

Koslow J. (2009). *The role of acoustics in ecosystem-based fishery management*. ICES Journal of Marine Science, 66: 966-973.

Kubecka J. and Wittingerova M. (1998). *Horizontal beaming as a crucial component of acoustic fish stock assessment in freshwater reservoirs*. Fisheries Research, 35: 99-106.

Lassen H. and Stæhr K. (1985). *Target strength of Baltic herring and sprat measured in situ.* ICES CM B, 41, 1-14.

Love, R. (1971). *Measurements of fish target strength: a review*. Fishery Bulletin, 69, 703-715.
MacLennan D., Fernandes P., and Dalen J. (2002). *A consistent approach to definitions and symbols in fisheries acoustics*. ICES Journal of Marine Science, 59: 365-369.

McClatchie S., Alsop J., and Coombs R. (1996). *A re-evaluation of relationships between fish size, acoustic frequency, and target strength*. ICES Journal of Marine Science, 53: 780-791.

McHugh J. (1972). *Marine fisheries of New York State*. Fishery Bulletin, 70(3): 585-610.
Nicholson W. (1978). *Movements and population structure of Atlantic menhaden indicated by tag returns*. Estuaries, 1, 141-150.

Nakken O. and Olsen K. (1977). *Target-strength measurements of fish*. Rapports et Procès-Verbaux des Réunions du Conseil International pour l'Exploration de la Mer. 170: 52-69.

Nicholson, W. (1978). *Movements and population structure of Atlantic menhaden indicated by tag returns.* Estuaries, 1: 141-150.

Northeast Fisheries Science Center (NEFSC). (2006). *42nd northeast regional stock assessment workshop (42nd SAW)*. NEFSC Reference Document, 06-09b. 308 pp.

Overholtz W., Jech M., Michaels W., and Jacobson L. (2006). *Empirical comparisons of survey designs in acoustic survey designs in acoustic surveys of Gulf of Maine-Georges Bank Atlantic herring*. Journal of Northwest Atlantic Fishery Science, 36: 127-144.

Petitgas P., Reid D., Carrera P., Iglesias M., Georgakarakos S., Liorzou B., and Masse J. (2001). *On the relation between schools, clusters of schools, and abundance in pelagic fish stocks*. ICES Journal of Marine Science, 58: 1150-1160.

Quinlan J., Blanton B., Miller T., and Werner F. (1999). *From spawning grounds to the estuary: using linked individual-based and hydrodynamic models to interpret patterns and processes in the oceanic phase of Atlantic menhaden Brevoortia tyrannus life history.* Fisheries Oceanography, 8: 224-226.

Reintjes, J. (1969). *Synopsis of biological data on the Atlantic menhaden, Brevoortia tyrannus*. U.S. Department of the Interior Fish and Wildlife Service. FAO Species Synopsis No. 42(Circul. 320): 0-30.

Rice J., Quinlan J., Nixon S., Hettler W., Warlen S., and Stegmann P. (1999). *Spawning and transport dynamics of Atlantic menhaden: Inferences from characteristics of immigrating larvae and predictions of a hydrodynamic model*. Fisheries Oceanography, 8: 93-110.

Robertis A. and Higginbottom I. (2007). *A post-processing technique to estimate the signal-to-noise ratio and remove echosounder background noise*. ICES Journal of Marine Science, 64: 1282-1291.

Rose G., Gauthier S., and Lawson G. (2000). *Acoustic surveys in the full monte: simulating uncertainty*. Aquatic Living Resources, 13: 367-372.

Rudstam L., Parker S., Einhouse D., Witzel L., Warner D., Stritzel J., Parrish D., and Sullivan P. (2003). *Application of in situ target-strength estimations in lakes: examples from rainbow-smelt surveys in Lakes Erie and* . ICES Journal of Marine Science, 60: 500-507.

Sanchirico J., Smith M., and Lipton D. (2007). *An empirical approach to ecosystem-based fishery management*. Ecological Economics, 64: 586-596.

Senate Document, No. 49, 45th Cong., 2nd sess. (1878).

Simmonds E. and MacLennan D. (2006). *Fisheries acoustics: Theory and practice,* (2nd ed.). Oxford, UK: Blackwell.

Shen H., Quinn T., Wespestad V., Dorn M., and Kookesh M. (2008). *Using acoustics to evaluate the effect of fishing on school characteristics of Walleye Pollock*. Resiliency of Gadid Stocks to Fishing and Climate Change, Alaska Sea Grant, University of Alaska Fairbanks: 125-140.

Sigler M. and Scepp D. (2007). *Seasonal abundance of two important forage fish species in the North Pacific Ocean, Pacific herring and walleye pollock*. Fisheries Research, 83: 319-331.

Skern-Maruitzen M., Otterson G., Handergard N., Dingsor G., Stenseth N., and Kjesbu O. (2015). *Ecosystem processes are rarely included in tactical fisheries management*. Fish and Fisheries, 1: 165-175.

Smith J. (1991). *The Atlantic and Gulf menhaden purse seine fisheries: Origins, harvesting technologies, biostatistical monitoring, recent trends in fisheries statistics, and forecasting.* Marine Fisheries Review, 53: 28-41.

Smith J. (1999). *Distribution of Atlantic menhaden, Brevoortia tyrannus, purse-seine sets and catches from southern New England to North Carolina, 1985-96.* NOAA Technical Report NMFS 144, 26 pp.

Smith J., O'Bier B., and McNeil N. (2008). *Length and weight relationships for Atlantic menhaden, Brevoortia tyrannus*. Journal of the North Carolina Academy of Science, 124:102-105.

Southeast Data, Assessment, and Review (SEDAR). (2015). *SEDAR 40 – Atlantic menhaden stock assessment report*. SEDAR, North Charleston, SC. http://www.asmfc.org/uploads/file/55089931S40_AtlMenhadenSAR_CombinedFINAL_1.15.2015-reduced.pdf

Suffolk County Department of Health Services. (2016). *Investigation of fish kills occurring in the Peconic river – Riverhead, N.Y. spring 2015,* Great River, NY.

Taylor B. and Kuyatt C. (1994). *Guidelines for evaluating and expressing the uncertainty of NIST measurement results.* Gaithersburg, MD: U.S. Department of Commerce.

Thomas G., Kirsh J., and Thorne R. (2002). *Ex situ target strength measurements of Pacific herring and Pacific sand lance*. North America Journal of Fisheries Management, 22: 1136-1145.

Trenkel V., Ressler P., Jech M., Giannoulaki M., and Taylor C. (2011). *Underwater acoustics for ecosystem-based management: State of the science and proposals for ecosystem indicators*. Marine Ecology Progress Series, 442: 285-301.

Turrentine J. (1913). *The menhaden industry*. Industrial and Engineering Chemistry, 5: 378-388.

Uphoff J. (2003). *Predator-prey analysis of striped bass and Atlantic menhaden in upper Chesapeake Bay*. Fisheries Management and Ecology, 10: 313-322.

Vaughan D., Prager M., and Smith J. (2002). *Consideration of uncertainty in stock assessment of Atlantic menhaden*. American Fisheries Society Symposium, 27: 83-112.

Wall C., Gobler C., Peterson B., and Ward J. (2013). *Contrasting growth patterns of suspension-feeding molluscs (Mercenari mercenaria, Crassostrea virginica, Argopecten irradians, and Crepidula fornicate) across a eutrophication gradient in the Peconic Estuary, NY, USA.* Estuaries and Coasts, 36: 1274-1291.

Weber A. and Grahn C. (1995). *Commercial finfish and crustacean landings from Peconic and Gardiners Bay, New York 1980-1992*. New York State Department of Environmental Conservation, Division of Marine Resources, Bureauof Finfish and Crustaceans, 24 pp.

Weber A., Grahn C., and Havens B. (1998). *Species composition, seasonal occurrence and relative abundance of finfish and macroinvertebrates taken by small-mesh otter trawl in Peconic Bay, New York.* New York State Department of Environmental Conservation, Division of Fish, Wildlife and Marine Resources, Marine Finfish Unit. 127 pp.